Development and validation of polygenic scores for within-family prediction of disease risks

Spencer Moore[1], Ivan Davidson[1], Jonathan Anomaly[1], Jeremiah H. Li[1], Mohammad Ahangari[1], Lauren Moissiy[1], Michael Christensen[1], Alexander Strudwick Young[1,2], David Stern[1*], Tobias Wolfram[1*]

[1]Herasight Research, USA

[2]Human Genetics Department, UCLA David Geffen School of Medicine, Los Angeles, CA, US

[*]Contributed equally

Abstract

The clinical implementation of polygenic scores (PGSs) for disease risk prediction, particularly in reproductive health applications, requires rigorous validation. Here, we develop seventeen disease PGSs by conducting large-scale GWAS meta-analyses, and we validate our scores in out-of-sample prediction analyses. We achieve state-of-the-art predictive performance, consistently matching or outperforming academic and commercial benchmarks, with liability R^2 reaching up to 0.21 (type 2 diabetes). The performance of a PGS for embryo screening depends on its predictive ability within-family, which can be lower than its prediction ability among unrelated individuals. However, very few disease PGSs have been tested within-family. We perform systematic within-family validation of our disease PGSs, finding no decrease in predictive performance within-family for 16 of 17 scores. PGS performance typically declines with genetic distance from training data, an effect that needs to be accounted for to give properly calibrated predictions across ancestries. We perform extensive calibration of our scores' performance across different ancestries, finding improved cross-ancestry performance compared to previous approaches, especially in African and East Asian populations. This is likely due to the fact our scores are constructed using a method that incorporates functional genomic annotations on more than 7 million variants, enabling a degree of fine-mapping of causal variants shared across ancestries. We illustrate clinical utility through examining the risk reduction that could be achieved through embryo screening for type 2 diabetes: selecting among 10 embryos is expected to reduce absolute disease risk by 12-20% in families where both parents are affected, with similar relative risk reductions across ancestries. These findings establish a framework for implementing PGS in reproductive medicine while demonstrating both the technology's potential for disease prevention and the methodological standards required for responsible clinical translation.

Introduction

Disease polygenic scores (PGS) aim to quantify an individual's genetic liability for developing specific diseases over the course of his or her life[1]. The development of PGSs relies on genome-wide association studies (GWAS) that quantify the marginal association between primarily com-

mon genetic variants and the disease of interest. The collection of large cohorts with genetic and health data has enabled well-powered GWASs[2], leading to an increasing number of PGSs that attain useful predictive ability across traits and diseases[3].

PGSs have shown great promise for risk stratification for common diseases, including breast cancer and coronary artery disease. By 2018, breast cancer PGS identified nearly an order of magnitude more women at equivalent risk as those carrying classic monogenic risk alleles such as those in the BRCA1/2 genes[4]. Likewise, a coronary artery disease PGS—leveraging GWAS data from biologically related traits such as LDL—classified 20.0% of the population at 3-fold risk compared to the average[5]. Such results demonstrate the potential for PGSs to be used alongside conventional disease risk factors in risk stratification, with increasing awareness of their utility in informing clinical practice and preventative medicine[6,7,8].

However, most GWASs to date have relied heavily on European populations[9]. As a consequence, PGS often exhibit substantially reduced predictive performance when applied to genetically distant populations[10,11]. Although the underlying causal genetic architecture of traits appears to be broadly conserved across ancestries[12], this reduced portability poses both methodological challenges and bioethical concerns regarding the potential exacerbation of existing health disparities[13]. Addressing this issue requires diversifying study cohorts[14] and implementing improved statistical methods for cross-ancestry prediction[15].

Although the target of disease GWASs is estimation of direct genetic effects—effects of alleles in an individual on that individual, relevant for within-family prediction—the associations also include contributions from factors not relevant to within-family prediction: indirect genetic effects through the family environment ("genetic nurture"[16]) and confounding from population stratification and assortative mating[17]. These factors can lead to attenuation of PGS prediction ability within-families. Although behavioral and social science genetics increasingly quantify and address these biases through within-family designs[18,19], medical genetics typically neglects such controls[20], presuming their irrelevance to biologically proximal traits. Consequently, disease PGS are rarely validated within families, with existing studies either focusing primarily on non-disease traits[19] or inadequately measuring within-family attenuation[21,22]. Furthermore, recent large-scale family-GWAS have revealed imperfect correlations between direct genetic effects for biomedical and disease traits compared to standard population effects (as estimated by non-family-based GWAS), challenging prevailing assumptions[23].

This is of particular importance for the application of PGS in the context of polygenic embryo screening (preimplantation genetic testing for polygenic traits, PGT-P), which uses genome-wide data to predict embryos' genetic risk for complex diseases, and which has garnered attention due to its potential to substantially reduce lifetime disease burden[24]. The disease risk reduction in PGT-P is primarily determined by the direct effect of a PGS (i.e., its association with the trait or disease within-family[25]). Without stringent validation, including estimation of the PGS direct effect within-family, no trustworthy statement on the utility of a PGS for embryo screening can be made.

Despite these methodological concerns, comprehensive validations of state-of-the-art disease PGS remain scarce. Existing studies seldom systematically benchmark PGS across multiple ancestries, and none employ within-family validation strategies to distinguish direct genetic effects from population-level confounding. To address these gaps, we constructed seventeen disease PGS using state-of-the-art methods aiming at maximising prediction ability, and we rigorously assessed their predictive performance in both population-based and within-family contexts. Ad-

ditionally, we quantify the attenuation of predictive accuracy along the genetic ancestry continuum. Using consistent metrics, we benchmark our newly developed PGS against existing state-of-the-art academic and commercial scores, finding that our models achieve either superior or statistically equivalent performance. Finally, leveraging the validated within-family predictive ability, we illustrate the practical implications of our approach by demonstrating the potential risk reduction achievable through embryo screening using our type 2 diabetes (T2D) PGS.

Results

PGS performance between and within families with genetically inferred European ancestries

We constructed a set of seventeen disease PGSs using a curated set of GWAS summary statistics generated by meta-analyzing individual GWAS studies from FinnGen[26], the Million Veterans Program (MVP)[27], the Global Biobank Meta-analysis Initiative (GBMI)[28], trait-specific consortia and the UK Biobank (UKBB)[29]. For UKBB in particular, we ran GWAS on a subset of self-reported white British individuals with genetically inferred Northwestern European ancestry (hereafter the 'United Kingdom' group), holding out related individuals and small test sets for later use in PGS validation. We used SBayesRC[30], a method that uses genomic annotations to improve effect estimates, to construct our PGSs.

Performance was initially evaluated using a held-out sample of UKBB individuals genetically inferred to have predominantly European ancestries, using relevant disease outcomes ascertained via electronic health records and self reported disease status (**Supplementary Table 1**). For these validations and for later comparisons, predictive performance was evaluated as liability R^2, or the proportion of variance explained on an underlying, continuous measure of disease predisposition. This quantity relies on the liability threshold model of disease, whereby those with liability exceeding that corresponding to a given population prevalence are considered cases. Among the evaluated PGSs, the highest predictive performance was observed for prostate cancer, type 2 diabetes (T2D), hypertension, and Alzheimer's disease (AD) (**Figure 1A**, **Supplementary Table 2**). The superior performance of these PGSs can be attributed to distinct factors. T2D and hypertension, which are highly polygenic traits, had the largest effective GWAS sample sizes in our analysis (**Table 1**). Complex diseases demonstrate extensive polygenicity[31,32,33], whereas cancers, while still polygenic, typically show lower degrees of polygenicity[34]. Prostate cancer demonstrated the highest predictive accuracy among malignancies, corresponding to its larger GWAS sample size relative to other cancers (**Table 1**). Similarly, the exceptional performance of the AD PGS is likely attributable to the presence of the APOE $\varepsilon 4$ haplotype with an unusually large effect size for complex diseases, which confers a 2–3 fold increased risk with one copy and 10–15 fold increased risk with two copies[35]. These findings suggest that both GWAS sample size and the genetic architecture of traits are primary determinants of PGS predictive performance[36].

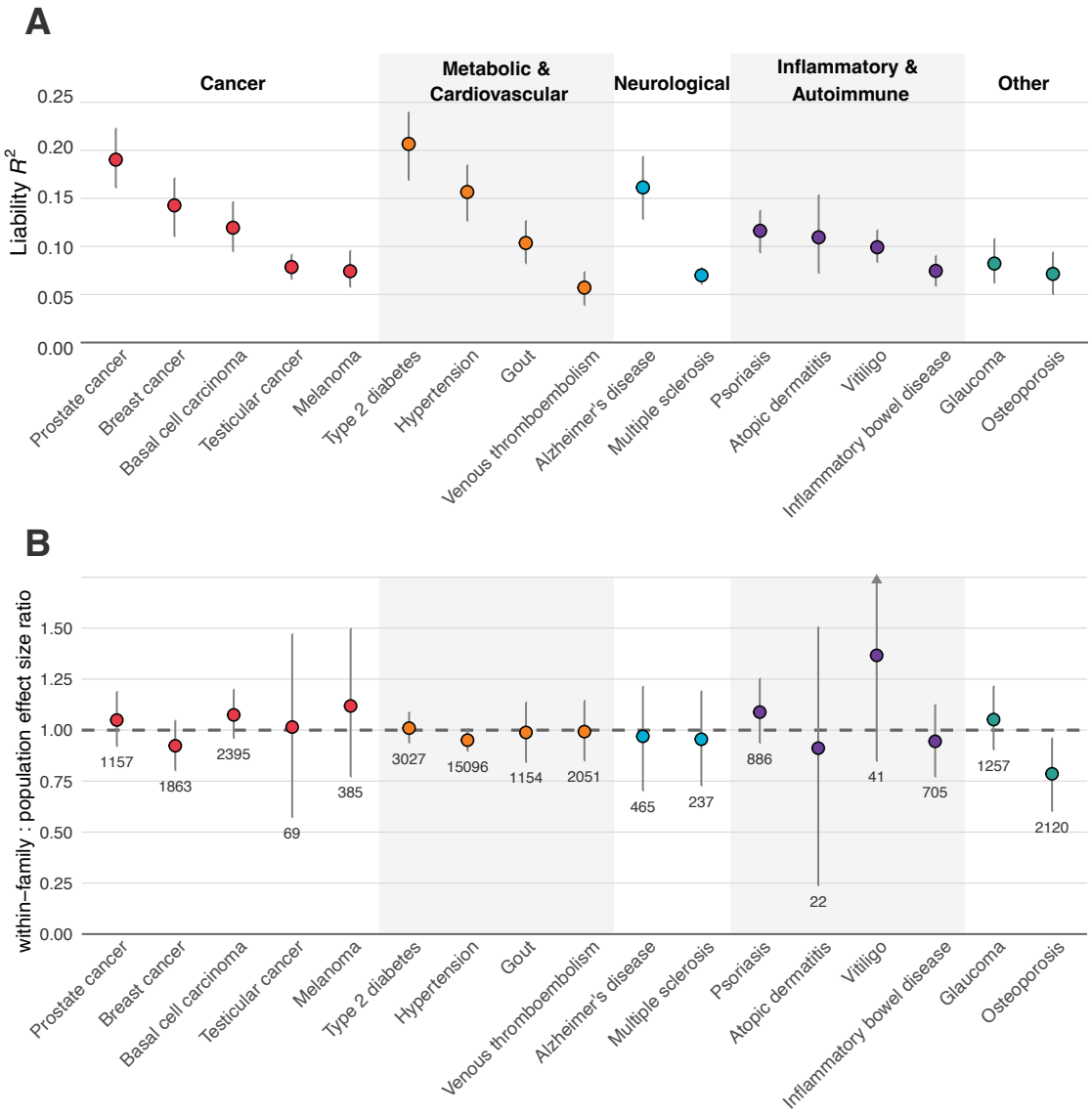

Figure 1: **Fraction of the variance in disease liability explained by PGSs between and within families in UK Biobank.**

A) Variance explained in disease liability by its corresponding PGS on the liability scale. B) The ratio of effect sizes observed in population and within-family regression analyses in identical samples, where the dotted line at 1 indicates identical strength of association between and within families. The numbers below the point estimates indicate the number of probands identified in UKBB as cases. Bands indicate bootstrapped 95% confidence intervals.

Disease	N cases	N control	Effective N
Vitiligo	2,853	37,405	10,603
Testicular cancer	9,885	302,233	37,550
Gout	11,472	360,137	44,471
Multiple sclerosis	19,973	882,985	58,653
Psoriasis	23,362	393,072	69,768
Atopic dermatitis	25,996	397,093	90,164
Inflammatory bowel disease	34,125	438,013	93,862
Osteoporosis	27,078	744,249	103,764
Melanoma	34,431	795,873	107,205
Alzheimer's disease	35,565	646,311	129,587
Glaucoma	37,880	1,060,839	144,229
Venous thromboembolism	60,812	1,255,839	231,543
Prostate cancer	112,901	374,563	276,762
Basal cell carcinoma	80,110	1,132,732	299,181
Breast cancer	168,404	470,884	373,165
Hypertension	305,027	565,625	784,649
Type 2 diabetes	254,150	1,487,323	860,791

Table 1: **Effective sample size and composition of the GWAS data used in PGS training.** *Effective sample size was computed as the sum of per-study effective sample sizes following eq. (6) in Grotzinger et al.*[37] *Where input GWASs were themselves meta-analyses, cohort-level information was extracted to compute overall meta-analytic effective sample sizes. If such information was not available, recommendations from Tucker-Drob 2025*[38] *were instead implemented.*

To estimate direct genetic effects and evaluate the predictive validity of PGSs in an embryo screening context, we performed within-family analyses that control for parental genotypes. We leveraged first-degree relatives in the UK Biobank cohort to impute parental genotypes using the *snipar* package[18]. This approach enabled us to calculate PGSs for both focal individuals and their (imputed) parents, allowing us to evaluate the degree to which the previously observed effects were driven by direct genetic effects versus other factors.

We found that the within-family predictive power of the PGSs was not significantly different from the population-based associations for sixteen out of the seventeen PGSs considered, with only the PGS for osteoporosis having a nominally significant lower within-family effect (**Figure 1B**). For the remaining PGSs, all point estimates of the ratio of within-family to population-based effect size estimates were greater than 0.9 and not significantly different from one ($P > 0.05$), suggesting that the predictive ability of these PGSs derives almost entirely from direct genetic effects (**Supplementary Table 6**).

Attenuation of PGS performance with increasing genetic distance from training cohorts

The reduced performance of PGSs in individuals with ancestries genetically distant from those used in the training GWAS is widely appreciated. This phenomenon is likely due to differences in the linkage disequilibrium structure of genomes with ancestry, with differences increasing with genetic distance, as well as other potential factors[10]. As the majority of GWASs conducted thus far have used samples of individuals with predominantly European genetic ancestries (including

those developed here), it is crucial to evaluate the performance reduction along the continuum of genetic ancestries.

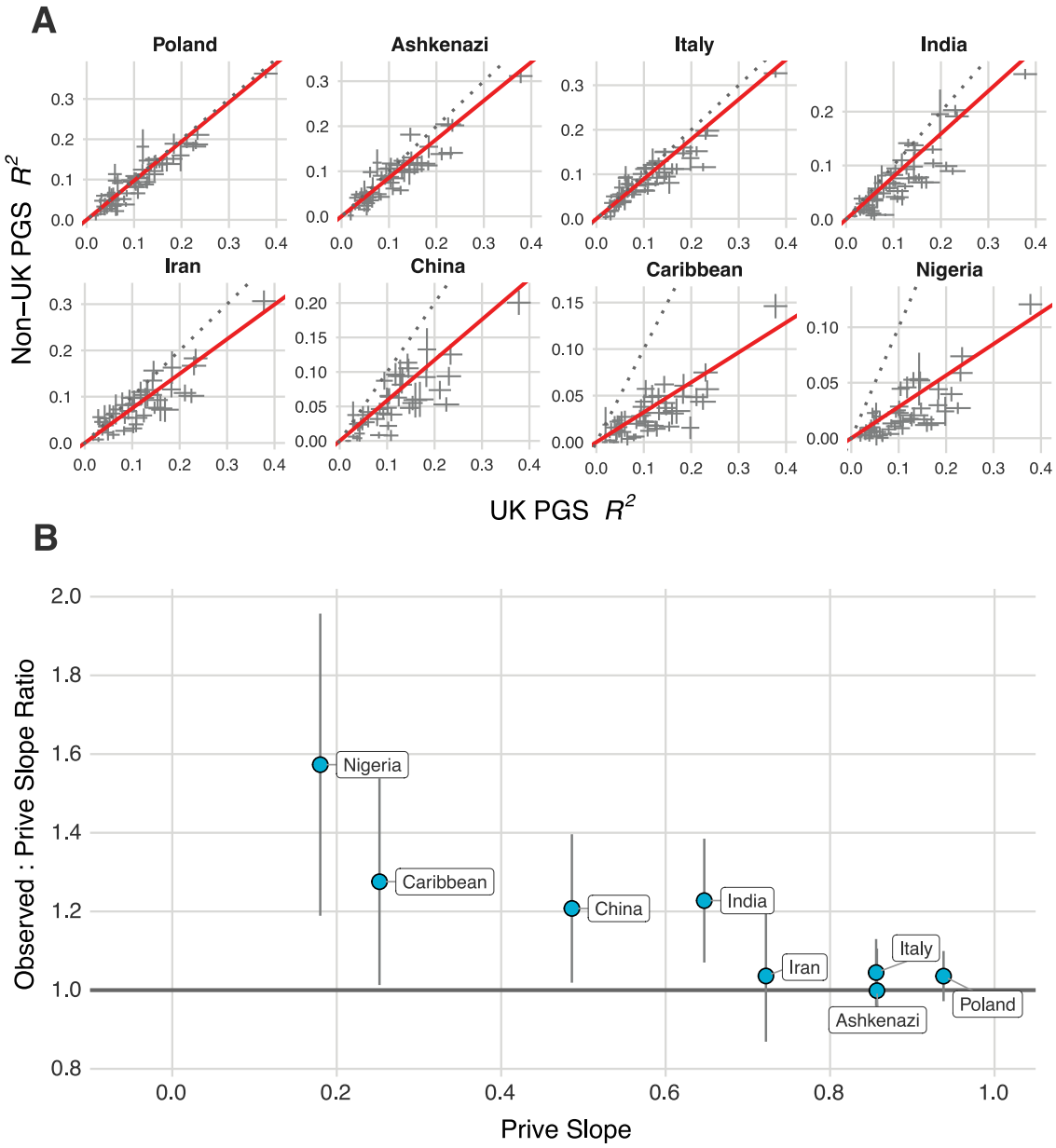

Figure 2: **PGS effect size attenuation across ancestries.**

A) Scatterplots showing the R^2 attained by a given PGS in the United Kingdom ancestry subsample on the x axis versus that attained in the given non-UK ancestry sample on the y axis. Intervals indicate standard errors, the red lines indicate the Deming regression slope (intercept fixed at 0), and the dotted gray line indicates the y=x line. See ***Table 2*** *for slope values and 95% confidence intervals. B) A scatterplot comparing the effect reduction slopes inferred from Prive et al.[10] versus the ratio of the slopes we observed in (A) to Prive et al. for the different groups analyzed. The intervals indicate standard errors for the Deming regression coefficients.*

Group	Deming regression slope (CI)	Prive et al. slope
Poland	0.971 (0.912, 1.03)	0.938
Italy	0.894 (0.821, 0.967)	0.856
India	0.794 (0.692, 0.896)	0.647
Iran	0.748 (0.627, 0.869)	0.722
Ashkenazi	0.856 (0.764, 0.948)	0.857
China	0.587 (0.495, 0.679)	0.486
Caribbean	0.321 (0.255, 0.388)	0.252
Nigeria	0.283 (0.214, 0.352)	0.180

Table 2: **Attenuation in PGS performance across ancestries.**
*Observed Deming regression slopes with 95 % confidence intervals for the regressions reported in **Figure 2** and corresponding slopes from Prive et al.*

To assess the reduction in PGS performance in samples of individuals with diverse genetic ancestries, we replicated the analyses introduced in Prive et al.[10] Firstly, we used an identical PGS generation pipeline as that used for the disease PGSs to generate around 40 to 80 PGSs — with the number varying depending on the sample size for each ancestry — for a variety of additional traits, including continuous biomarker traits for which PGS performance is more easily estimated (**Supplementary Table 1**). Secondly, we constructed a diverse set of eight discretized groups based on genetically-inferred ancestries, using reference panels of individuals with self-reported countries of origin (or religious affiliation in the case of Ashkenazi Jewish individuals). Specifically, we identified groups that genetically resembled self-reported individuals from Poland, Italy, Iran, India, China, the African Caribbean population and Nigeria and those identifying as being of Ashkenazi Jewish descent. Thirdly, we calculated the R^2 for each PGS (e.g., BMI, apolipoprotein A) in the UK Biobank United Kingdom ancestry group and compared it to the R^2 attained in each group. Finally, we regressed the R^2 attained in each group on the value attained in the UK Biobank United Kingdom ancestry group which allowed us to assess the performance reduction factor (**Figure 2A**).

We found that PGS performance decreased as the centroid of a given group in common variant PC space increased in distance from the centroid of the training GWAS data (**Figure 2**). Notably, we found that the relative attenuation in our PGS construction pipeline was less severe than that observed in Prive et al., observing significantly better performance particularly in the more genetically distant groups from the ancestries represented in the training GWASs (**Figure 2B**). This improvement in portability was likely due to the fact SBayesRC leverages genomic functional annotations that are independent of ancestry, enabling fine-mapping of causal loci, as the authors of SBayesRC similarly observed, albeit on a more limited set of traits[30].

Performance of PGS compared to academic and commercial entities

We next sought to compare the performance of the disease PGS we developed here to those developed by various academic groups and other commercial providers. Thompson et al. (2024)[39] and Mars et al. (2022)[40] generated several disease PGS that overlap with those generated here and reported the odds ratio associated with a one standard deviation increase in the PGS in UKBB and Finngen, respectively[26,29]. Across all scores where we could identify a comparable PGS-disease pair, we found that our scores outperformed or performed as well as those generated by Thompson et al. and Mars et al. (**Figure 3A**). We note substantially improved performance with respect to breast cancer, melanoma, gout, and multiple sclerosis, with our scores having higher point estimates across all disease with the exception of glaucoma, for which Thompson et al. reported a slightly higher though statistically indistinguishable odds ratio point estimate. Our liability R^2 was on average 28% and 87% higher than those of Thompson et al. and Mars et al., respectively. When compared to the liability R^2 reported by two commercial entities (assuming identical population prevalence), we similarly found the PGSs reported here showed substantially better performance: 122% better than Orchid and 193% better than Genomic Prediction on average (**Figure 3B**). In several cases, the point estimates suggest the PGSs we trained explain more than two times as much variance in disease liability as explained by the PGSs developed by other commercial entities. Notably, Orchid provided PGS validations for only five out of the 17 traits included here, and we were unable to determine appropriate confidence intervals for their reported performance metrics. When the documented validation methodology of a commercial entity was illegitimate or incompatible with ours, we omitted the score in question (e.g., validation results reported by Orchid for Alzheimer's disease are therefore not shown as the reported validation includes age as a covariate, which likely had an outsized contribution to their reported performance.)[41]. While we made extensive efforts to evaluate Nucleus Genomics, we were unable to reconcile their performance estimates with established theoretical and empirical boundaries of polygenic prediction, necessitating their exclusion from our primary analysis (see **Supplementary Note** for technical details)

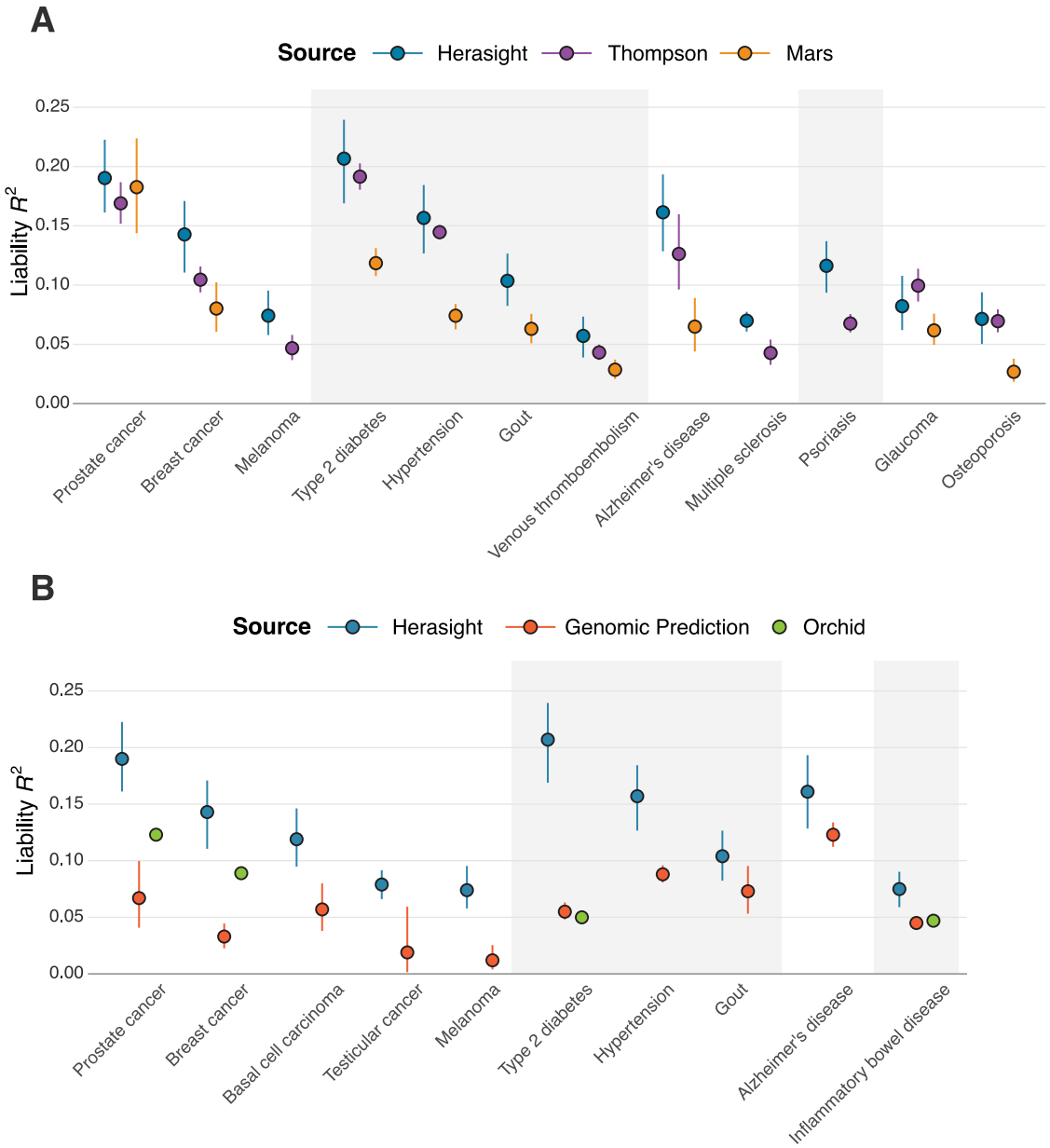

Figure 3: **Comparison of PGS performance to external academic and commercial entities.** *Variance explained in disease liability by its corresponding PGS on the liability scale, comparing results for PGS constructed in the current work by Herasight to those reported by A) two academic groups: Thompson et al. and Mars et al. and B) two commercial entities: Genomic Prediction and Orchid. Bands indicate bootstrapped 95% confidence intervals. Note that we were not able to ascertain 95% confidence intervals for Orchid. Equivalent population prevalences were used in the conversion to liability R^2 (see* ***Methods****).*

Case Study: The utility of polygenic embryo screening in reducing lifetime risk of T2D

To demonstrate the utility of our PGSs in the context of embryo screening, we used T2D polygenic screening as a case study. We calculated the expected absolute and relative risk reduction for type 2 diabetes in couples with varied continental genetic ancestries and disease status. These are calculated using mean expected attenuations based on centroids calculated in PC space. Since

the true attenuation for any given couple will doubtlessly vary, these calculations are largely illustrative. Even with as few as five embryos, the expected reduction in absolute risk for type 2 diabetes ranges from 5% to 15% depending on parental ancestries and disease status (**Figure 4**). If screening were applied to twenty embryos, the expected reduction in disease risk becomes substantial to the degree that when both parents are affected, the expected relative risk reduction ranges from 23% to 51% and absolute risk reduction ranges from 14% to 24% depending on parental ancestries.

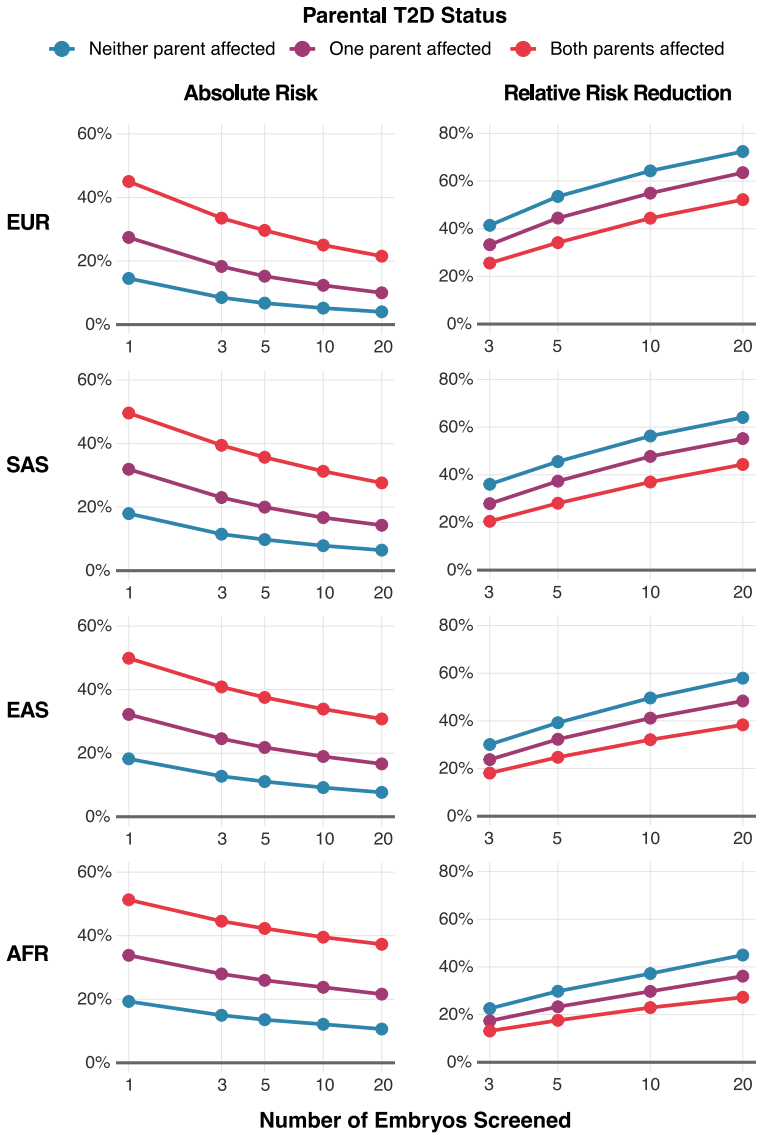

Figure 4: **Expected reduction in T2D risk with embryo screening using the Herasight PGS.**
We calculated the absolute lifetime risk (left) and relative risk reduction (right) parents with different continental ancestries could expect via embryo screening, under various scenarios of parental T2D affectation status and the number of screened embryos (see ***Methods****). Lifetime T2D risk estimates are reported in* ***Supplementary Tables 3 and 4****. EUR: European, SAS: South Asian, EAS: East Asian, AFR: African genetic ancestries.*

Another determinant of potential risk reductions is the predictive power of the PGS, which as noted above varies both by target disease and model developer. Table 3 displays absolute

and relative risk reductions for a hypothetical couple of European continental genetic ancestry in which either the father or mother is affected. Selection among five embryos in this scenario yields relative risk reductions exceeding 40% where PGS liability R^2 is high, but commensurately lower reductions of 21% to 36% where the PGS only captures a few percentage points of liability variance.

Disease	Company	PGS R^2 (%)	Population baseline (%)	Family baseline (%)	Absolute risk reduction (%)	Relative risk reduction (%)
Breast cancer	Herasight	14.3	13.9	19.8	8.1	41.0
	Orchid	8.8	13.9	19.8	6.4	32.3
	GP	3.3	13.9	19.8	4.1	20.6
Prostate cancer	Herasight	19.0	12.6	24.5	10.8	44.2
	Orchid	12.3	12.6	24.5	8.8	36.2
	GP	6.7	12.6	24.5	6.7	27.4
Type 2 diabetes	Herasight	20.7	21.4	27.5	12.1	43.8
	Orchid	5.0	21.4	27.5	6.1	22.0
	GP	5.5	21.4	27.5	6.6	23.8

Table 3: **Expected reduction in disease risk with embryo screening using validated PGS from providers of preimplantation genetic testing for polygenic diseases (PGT-P) (Herasight, Orchid, and Genomic Prediction (GP)).**
We calculated the absolute and relative risk reductions a couple of European continental genetic ancestry with one parent affected could expect when screening five embryos using various PGS models. Lifetime breast cancer, prostate cancer and T2D risk estimates are reported in ***Supplementary Table 3****. "Population baseline" refers to the risk pertaining to all families in the population and "Family baseline" only to those with one parent affected by the disease, which are therefore higher than the former for each disease.*

Conclusion

We have generated PGSs for seventeen diseases spanning several disease groups. We demonstrated state-of-the-art performance relative to academic and commercial benchmarks across diseases, attaining superior or statistically indistinguishable performance to other groups in all cases. Our work represents the first systematic within-family validation across multiple disease PGS at this scale, demonstrating that predictive accuracy is predominantly driven by direct genetic effects for sixteen of seventeen diseases evaluated. The exception, osteoporosis, serves as a proof of principle that PGS prediction of disease traits can exhibit reduced performance within-family due to confounding, underscoring the importance of within-family validation for any PGS intended for embryo screening. A PGS exhibiting reduced performance within-family can still be used for embryo screening, but the reduced prediction ability needs to be accounted for when calibrating predictions

By applying Bayesian mixture models to more than seven million SNPs while utilising genomic functional annotations[30], we observed improved cross-ancestry portability compared to previous approaches, with predictive accuracy maintained at higher levels in individuals genetically distant from the training data. Although this represents progress toward addressing disparities in PGS performance, achieving more equal accuracy across all ancestries remains a

central challenge requiring continued development of diverse cohorts and methodology.

Our results show that polygenic embryo screening holds promise for reducing disease risk, particularly when a family history of disease is present. As the T2D case study illustrates (**Figure 4**), the absolute risk reductions are most pronounced when one or both parents are affected. However, current PGS implementations, including ours, primarily capture common variant contributions to disease risk. Family history often additionally reflects the segregation of rare, high-effect variants that substantially influence disease liability but are not captured by PGSs. Comprehensive risk assessment in the embryo screening context will require integrated models that combine polygenic background from common variants, high-effect rare variants (particularly critical in families with strong disease history), and explicit family history information. The preimplantation genetic testing (PGT) setting presents unique methodological challenges for such integration, including constraints on DNA quantity from embryo biopsies and the need for accurate imputation and variant calling across the allele frequency spectrum. Future work should prioritize improving the calling of all classes of genetic variation in embryos, ultimately enabling more accurate risk stratification that reflects the full genetic architecture underlying disease risk.

Our findings suggest several directions for advancing the field. The consistent within-family performance across most diseases indicates that continued investment in larger, more diverse GWAS should yield direct benefits. The improved portability achieved through methodological enhancements demonstrates that technical innovation can help address existing disparities even with current data limitations. The validation approach presented here, encompassing population-based performance, within-family analyses, ancestry portability assessment, and systematic benchmarking, may serve as a useful framework as the field moves toward clinical implementation.

Important challenges remain in characterizing pleiotropic effects, integrating rare variant information, and ensuring sufficient performance across ancestries. Similarly, the probabilistic nature of polygenic risk requires careful communication strategies that contextualize individual PGS-predicted disease risk that appropriately considers relevant family history to produce calibrated absolute risk estimates, which our analyses suggest are inadequately executed by other commercial providers (see **Supplementary Note**).

Despite these challenges, our results suggest that polygenic embryo screening, when implemented with appropriate validation, offers meaningful potential for reducing disease risk in future generations. Continued methodological development, coupled with open reporting and rigorous validation, will be essential for realizing this potential while ensuring broad access.

Methods

UK Biobank

The UK Biobank (UKBB) is a large population-based study consisting of nearly 500,000 individuals with genotypes and linked health records recruited from 22 sites throughout the UK[14]. The array-based version of the dataset imputed by Wellcome Trust Centre for Human Genetics (WTCHG; UKBB field 22828) was used during the first phase of the present study consisting of the development of the PGS models. To ensure quality control of this version of the UKBB genotypic and phenotypic data, we excluded individuals with outlier heterozygosity (UKBB field 22027), ten or more third-degree relatives also present in the data and a genotype missingness

rate greater than 3%. To retain as much trait-associated variation as possible while minimizing artifacts, genetic variants were excluded only when either Hardy-Weinberg (HWE) p-value or MAF was less than 1×10^{-50} and 1%, respectively. The final set of included variants for use in UKBB GWAS consisted of 6,667,399 biallelic SNPs overlapping with those comprising the SBayesRC variant panel[30]. We used the whole-genome sequence-based version of the UKBB dataset for PGS model validation during the second phase of the present study. Samples retained after quality control of the imputed version of the dataset were likewise retained for use in this second phase. Minimal filtering of variants passing GraphTyper's FILTER field with AAScore $> .8$ and MAF $> .1\%$ resulted in a final set of 7,153,533 biallelic SNPs again overlapping with those comprising the SBayesRC variant panel.

UKBB ancestry inference

Ancestry of UKBB samples passing above sample and genotype filters was inferred using the country-of-origin method described in Prive et al.[10]. Specifically, we accessed pre-computed principal component (PC) centroids for the subsets of UKBB participants hailing from the Caribbean, China, India, Iran, Italy, Poland, Nigeria and the United Kingdom as well as that for self-reported Ashkenazi Jews. We then matched ancestries to these centroids by computing the Euclidean distance between the first 16 PCs of QC-passing samples and the seven ancestry centroids; samples were assigned to the country-of-origin group of the nearest centroid. Samples matched to the "United Kingdom" ancestry group were further filtered to those individuals also reporting "Caucasian" genetic grouping (UKBB field 22006) and "British" ethnic background (UKBB field 21000).

GWAS summary statistics and meta-analysis

To attain the largest possible discovery sample sizes for PGS training, we collated GWAS summary statistics from several classes of sources: recently published GWAS, trait-specific genomics consortia, GBMI[28], FinnGen[26], healthcare registry GWAS, and internally-run UKBB GWAS. In cases where summary statistics were not immediately available, corresponding authors were contacted for provision of UKBB-left-out data and were acknowledged where re-analysis was required.

All summary statistics files were first harmonized to GRCh37 and corrected for errors in per-SNP sample size[42] following the recommendations from Tucker-Drob (2025)[38], using cohort-level information where possible. Corrected summary statistics files were then meta-analyzed with inverse variance weighting in METAL[43] where LDSC-estimated[44] genetic correlations between the available sources exceeded ~ 0.8. Where possible, UKBB GWAS were run with either REGENIE[45] or fastGWA[46] on a discovery sample consisting only of United Kingdom ancestry samples not overlapping with pre-selected test sets.

Construction of PGS

Internal PGS were built by providing our meta-analytic summary statistics as input to SBayesRC[30], a recently published Bayesian method leveraging information from functional genomic annotations. Training consisted of two stages: a first stage to perform basic quality control on input association statistics and to impute associations from untested SNPs as well as a second stage

to perform Markov Chain Monte Carlo parameter estimation. Resulting scoring files included weights from the $\sim$ 7.3M SNPs comprising the SBayesRC variant set provided by the authors of the method.

Literature-derived lifetime risk estimates

Lifetime risk estimates were estimated using available measures of lifetime risk, lifetime prevalence, and cumulative incidence. Data were collected from the National Cancer Institute's Surveillance, Epidemiology, and End Results (SEER) Program[47], Global Burden of Disease Study[48], CDC[49], and various other sources (see **Supplementary Tables 3** and **4**). In many cases multiple measures of lifetime risk were averaged. Population prevalence estimates were taken as the average of the male and female prevalence estimates for conditions that present in both sexes.

PGS validation and conversion of observed to liability R^2

Polygenic scores (PGS) were evaluated in R with the `lm()` function from the R *stats* package. For continuous traits we fit ordinary least-squares models in 1,000 unrelated UK Biobank participants of "United Kingdom" genetic ancestry, adjusting for age and the first ten PCs. For diseases with sufficient numbers of cases to permit test-set exclusion and an internal UKBB GWAS, PGS were validated in test sets consisting of 600 UKBB cases and 1,000 UKBB controls using a linear probability model (`lm()` on a 0/1 outcome) with PGS residualized on age and the first ten PCs. The estimated observed R^2 from these models was then converted to liability R^2 using the transformation of Lee et al.[50] ("*Observed-scale* $R_o^2 \rightarrow$ *liability-scale* R_l^2" in **Supplementary Table 5**). Standard errors were bootstrapped with 2,000 replicates.

Within-family PGS validation

Additional PGS validations were performed in the subset of UKBB participants for whom genotypes of at least one other parent or sibling were also available to permit Mendelian imputation of parental genotypes using the *snipar* package[18]. Such samples were identified using KING[51] and filtering to non-monozygotic relatives belonging to the United Kingdom ancestry group. In total 40,943 probands were included in the analysis. Variants were further filtered to those amenable to *snipar*-based genotype imputation with INFO > 0.99, resulting in a reduced set of 4,065,217 biallelic SBayesRC SNPs for within-family PGS scoring.

Binary outcomes were analysed with logistic regression, fitted in R via the *lme4* package `glmer()` function using the binomial probit link and modeling phenotypic correlations between siblings by fitting family-wise random intercepts. A first "population" model regressed the phenotype on age, sex, the third and fourth principal components as well as offspring PGS; a second "within-family" specification added the maternal and paternal snipar-imputed parental PGSs to separately estimate the non-transmitted component following the model introduced by Young et al. (2022, Equation 1)[18] (estimated population effects, direct effects, average NTCs and spousal PGS correlations are reported in **Supplementary Table 6**). To estimate the attenuation of PGS performance within-family, the ratio of the offspring PGS coefficients from the within-family and the population models was calculated for each trait and its standard error approximated via family-wise bootstrap with 2000 replicates.

Relative performance estimation

Relative performances were computed as the slope of a Deming regression of estimated variance explained in each non-"United Kingdom" group on that of the "United Kingdom" group for each trait. Regressions consisted of around 40 to 80 pairs of PGS performance estimates for the focal traits and diseases listed in **Supplementary Table 1**.

Comparison of PGS performances against those of academic PGS developers

To benchmark our PGS validation results against those previously reported in the academic literature, we extracted and converted performances recently published in Thompson et al. and Mars et al., which develop and validate PGS in UKBB and FinnGen, respectively. Performances from the former are provided in the publication's supplementary Table S3: Performance (disease) and in Table S4 of the latter. Both sources reported performances as odds ratios per standard deviation of PGS, which were converted to liability R^2 using known conversions (i.e., by sequentially applying the "*Odds-ratio per 1 SD of PGS (OR)* $\rightarrow$ *Cohen's d*", "*Cohen's d* $\rightarrow$ *observed-scale* R_o^2" and "*Observed-scale* R_o^2 $\rightarrow$ *liability-scale* R_l^2" conversions shown in **Supplementary Table 5** using the trait-specific lifetime risks and sample prevalences given in **Supplementary Tables 3**).

Comparison of PGS performances against those of commercial PGS for PGT-P providers

We likewise benchmarked our results against those previously claimed by commercial providers of PGS. Given a growing emphasis on the use of PGS for PGT-P, we extracted performances published online in whitepapers by Orchid Health[52] and by Genomic Prediction (now Lifeview) as Widen et al.[21], acknowledging that Genomic Prediction has since displayed risk reductions for a new PGS set whose validation performances have not been made public[53]. Both sources reported performances as AUROC, but only the latter computed parameter uncertainties. Reported values were converted to liability R^2 using known conversions (i.e., by sequentially applying the "*Area under ROC curve (AUC)* $\rightarrow$ *Cohen's d*", "*Cohen's d* $\rightarrow$ *observed-scale* R_o^2" and "*Observed-scale* R_o^2 $\rightarrow$ *liability-scale* R_l^2" conversions shown in **Supplementary Table 5** using the trait-specific lifetime risks and sample prevalences given in **Supplementary Tables 3** and **7**, respectively). For breast cancer, type 2 diabetes and inflammatory bowel disease, Orchid also reported performance as odds ratios per standard deviation of PGS, which was used for conversion to liability R^2 in place of an incomparable AUC metric computed using both PGS and additional covariates. In particular, the inclusion of age as an additional covariate in Orchid's sole published benchmark for Alzheimer's disease likely inflated the resulting AUC, precluding meaningful comparison between this and otherwise comparable estimates.

Simulations of expected gains from use of PGS models in PGT-P

Absolute and relative risk reductions achievable when applying the T2D PGS model in PGT-P were determined via simulation following the family-based variance decomposition first developed and implemented by Lencz et al.[24] Specifically, the portion of the genetic component captured by the PGS and shared between embryos was drawn as $C \sim \mathcal{N}\left(\mu_C, \frac{R^2_{\text{PGS}}}{2}\left(1 - \frac{R^2_{\text{PGS}}}{h^2}\right)\right)$ with R^2_{PGS} reduced according to the estimated relative performances corresponding to the parental ancestries (e.g., R^2_{PGS} reduced from $R^2_{\text{PGS:EUR/EUR}} = 20.7\%$ to $R^2_{\text{PGS:EUR/AFR}} = (20.7\% + .32 \times$

20.7%)/2 = 13.7% and $R^2_{\text{PGS:EAS/EAS}} = .59 \times 20.7\% = 12.2\%$ for a EUR/AFR couple and an EAS/EAS couple, respectively). μ_C depended on the average full genetic components of the parents (g_m and g_f) and the trait heritability such that $\mu_C = R^2_{\text{PGS}}/h^2 \times (g_m + g_f)/2$. In turn, g_m and g_f were allowed to separately depend on each parent's disease status, ancestry- and sex-specific lifetime risk of disease and the disease heritability. These were obtained via accept–reject sampling (ratio-of-uniforms implementation). The portion of the genetic component captured by the PGS and unshared between embryos was accordingly drawn as $X \sim N(0, R^2_{\text{PGS}}/2)$ and the full PGS for each embryo computed as $\text{pgs} = x + c$. The uncaptured, unshared genetic component $G_{\text{res}} \sim N(0, (h^2 - R^2_{\text{PGS}})/2)$ and the environmental residual $E_{\text{res}} \sim N(0, 1 - h^2)$ were then added to the full average parental genetic component, the unshared, captured genetic component and the environmental residual to compute the corresponding disease liability for each embryo (i.e., $l = (g_m + g_f)/2 + g_{\text{res}} + x + e$). Embryos were designated as disease cases where liability exceeded the disease threshold $T = \Phi^{-1}(1 - K)$, which in turn depended on embryos' ancestry- and sex-specific lifetime risk of disease K.

Embryo PGS, liability and disease status were simulated in 150,000 batches of 3, 5, 10 and 20 embryos for each unique combination of parental ancestries, parental disease status (i.e., father and/or mother affected) and batch size (400 unique combinations in total). Simulated prevalence of disease with and without selection was computed as the fraction of diseased embryos with the lowest PGS in each batch ($P_{\text{selection}}$) and the overall fraction of diseased embryos ($P_{\text{population}}$), respectively. Absolute risk reductions were then calculated as $P_{\text{population}} - P_{\text{selection}}$ and relative risk reductions as $(P_{\text{population}} - P_{\text{selection}})/P_{\text{population}}$.

Inference of implied liability variance explained from risk predictions

To quantify the implied performance of a PGS from disease risk predictions, we applied the liability threshold model to infer the liability variance explained (liability R^2 or R^2_l) from combinations of PGS z-scores, population prevalence, and predicted individual risk. Under the liability threshold model, disease liability L is modeled as $L = G + E$, where G represents the genetic component distributed as $G \sim N(0, R^2_l)$, E represents the environmental component distributed as $E \sim N(0, 1 - R^2_l)$, and G and E are assumed to be uncorrelated.

For a binary disease trait with population prevalence K, the liability threshold T is defined as $T = \Phi^{-1}(1 - K)$, where Φ^{-1} denotes the inverse standard normal cumulative distribution function. The probability of disease for an individual with standardized PGS value g is given by:

$$P(\text{Disease} \mid \text{PGS} = g) \;=\; \Phi\left(\frac{g\,R_l - T}{\sqrt{1 - R^2_l}}\right) \tag{1}$$

To infer the implied R^2_l from reported risk predictions, we solved numerically for the value of R^2_l that satisfies:

$$\Phi\left(\frac{g\,R_l - T}{\sqrt{1 - R^2_l}}\right) \;-\; P_{\text{reported}} \;=\; 0 \tag{2}$$

where P_{reported} represents the individual disease risk reported for an individual. This equation was solved using bisection root-finding with tolerance 10^{-12}, implemented in R. This approach enabled us to quantify the predictive performance implicitly claimed by risk predictions made for a given individual.

Acknowledgements

GWAS summary statistics

We thank the following individuals and groups: the Type 2 Diabetes Global Genomics Initiative (T2DGGI) for generation of association summary statistics without UKBB; the International Multiple Sclerosis Genetics Consortium (IMSGC) for provision of GWAS summary statistics; the participants and investigators of the FinnGen study; all other authors of GWAS used in PGS training for upholding data sharing norms in the GWAS field.

Datasets

This research has been conducted using the UK Biobank Resource under Application Number #103244. This work uses data provided by patients and collected by the NHS as part of their care and support.

Author contributions

Spencer Moore: Conceptualization; Data curation; Formal analysis; Software; Visualization; Writing — original draft; Writing — review & editing

Ivan Davidson: Investigation; Writing — review & editing

Jonathan Anomaly: Writing — review & editing

Jeremiah H. Li: Writing — review & editing

Mohammad Ahangari: Writing — review & editing

Lauren Moissiy: Writing — review & editing

Michael Christensen: Supervision; Project administration; Funding acquisition; Writing — review & editing

Alexander Strudwick Young: Methodology; Writing — review & editing

David Stern: Conceptualization; Methodology; Visualization; Supervision; Writing — review & editing

Tobias Wolfram: Conceptualization; Methodology; Supervision; Project administration; Writing — review & editing

References

[1] Lewis Cathryn M., Vassos Evangelos. Polygenic Risk Scores: From Research Tools to Clinical Instruments *Genome Medicine.* 2020;12:44.

[2] Abdellaoui Abdel, Yengo Loic, Verweij Karin J. H., Visscher Peter M.. 15 Years of GWAS Discovery: Realizing the Promise *The American Journal of Human Genetics.* 2023;110:179–194.

[3] Lambert Samuel A., Gil Laurent, Jupp Simon, et al. The Polygenic Score Catalog as an Open Database for Reproducibility and Systematic Evaluation *Nature Genetics.* 2021;53:420–425.

[4] Khera Amit V., Chaffin Mark, Aragam Krishna G., et al. Genome-Wide Polygenic Scores for Common Diseases Identify Individuals with Risk Equivalent to Monogenic Mutations *Nature Genetics.* 2018;50:1219–1224.

[5] Patel Aniruddh P., Wang Minxian, Ruan Yunfeng, et al. A Multi-Ancestry Polygenic Risk Score Improves Risk Prediction for Coronary Artery Disease *Nature Medicine.* 2023;29:1793–1803.

[6] Fuat Ahmet, Adlen Ella, Monane Mark, et al. A Polygenic Risk Score Added to a QRISK®2 Cardiovascular Disease Risk Calculator Demonstrated Robust Clinical Acceptance and Clinical Utility in the Primary Care Setting *European Journal of Preventive Cardiology.* 2024;31:716–722.

[7] Lennon Niall J., Kottyan Leah C., Kachulis Christopher, et al. Selection, Optimization and Validation of Ten Chronic Disease Polygenic Risk Scores for Clinical Implementation in Diverse US Populations *Nature Medicine.* 2024;30:480–487.

[8] Siena Leonardo Maria, Baccolini Valentina, Riccio Marianna, et al. Weighing the Evidence on Costs and Benefits of Polygenic Risk-Based Approaches in Clinical Practice: A Systematic Review of Economic Evaluations *The American Journal of Human Genetics.* 2025:S0002929725001934.

[9] Mills Melinda C., Rahal Charles. The GWAS Diversity Monitor Tracks Diversity by Disease in Real Time *Nature Genetics.* 2020;52:242–243.

[10] Privé Florian, Aschard Hugues, Carmi Shai, et al. Portability of 245 Polygenic Scores When Derived from the UK Biobank and Applied to 9 Ancestry Groups from the Same Cohort *The American Journal of Human Genetics.* 2022;109:12–23.

[11] Ding Yi, Hou Kangcheng, Xu Ziqi, et al. Polygenic Scoring Accuracy Varies across the Genetic Ancestry Continuum *Nature.* 2023;618:774–781.

[12] Hou Kangcheng, Ding Yi, Xu Ziqi, et al. Causal Effects on Complex Traits Are Similar for Common Variants across Segments of Different Continental Ancestries within Admixed Individuals *Nature Genetics.* 2023;55:549–558.

[13] Martin Alicia R., Kanai Masahiro, Kamatani Yoichiro, Okada Yukinori, Neale Benjamin M., Daly Mark J.. Clinical Use of Current Polygenic Risk Scores May Exacerbate Health Disparities *Nature Genetics.* 2019;51:584–591.

[14] Duncan L., Shen H., Gelaye B., et al. Analysis of Polygenic Risk Score Usage and Performance in Diverse Human Populations *Nature Communications.* 2019;10:3328.

[15] Kachuri Linda, Chatterjee Nilanjan, Hirbo Jibril, et al. Principles and Methods for Transferring Polygenic Risk Scores across Global Populations *Nature Reviews Genetics.* 2024;25:8–25.

[16] Kong Augustine, Thorleifsson Gudmar, Frigge Michael L., et al. The Nature of Nurture: Effects of Parental Genotypes *Science.* 2018;359:424–428.

[17] Young Alexander Strudwick. Estimation of Indirect Genetic Effects and Heritability under Assortative Mating 2023.

[18] Young Alexander I., Nehzati Seyed Moeen, Benonisdottir Stefania, et al. Mendelian Imputation of Parental Genotypes Improves Estimates of Direct Genetic Effects *Nature Genetics.* 2022;54:897–905.

[19] Alemu Robel, Terskaya Anastasia, Howell Matthew, et al. An Updated Polygenic Index Repository: Expanded Phenotypes, New Cohorts, and Improved Causal Inference 2025.

[20] Wang Ying, Tsuo Kristin, Kanai Masahiro, Neale Benjamin M., Martin Alicia R.. Challenges and Opportunities for Developing More Generalizable Polygenic Risk Scores *Annual Review of Biomedical Data Science.* 2022;5:293–320.

[21] Widen Erik, Lello Louis, Raben Timothy G., Tellier Laurent C. A. M., Hsu Stephen D. H.. Polygenic Health Index, General Health, and Pleiotropy: Sibling Analysis and Disease Risk Reduction *Scientific Reports.* 2022;12:18173.

[22] Lello Louis, Raben Timothy G., Hsu Stephen D. H.. Sibling Validation of Polygenic Risk Scores and Complex Trait Prediction *Scientific Reports.* 2020;10:13190.

[23] Tan Tammy, Jayashankar Hariharan, Guan Junming, et al. Family-GWAS Reveals Effects of Environment and Mating on Genetic Associations 2024.

[24] Lencz Todd, Backenroth Daniel, Granot-Hershkovitz Einat, et al. Utility of Polygenic Embryo Screening for Disease Depends on the Selection Strategy *eLife.* 2021;10:e64716.

[25] Bates Timothy C., Maher Brion S., Medland Sarah E., et al. The Nature of Nurture: Using a Virtual-Parent Design to Test Parenting Effects on Children's Educational Attainment in Genotyped Families *Twin Research and Human Genetics.* 2018;21:73–83.

[26] Kurki Mitja I., Karjalainen Juha, Palta Priit, et al. FinnGen Provides Genetic Insights from a Well-Phenotyped Isolated Population *Nature.* 2023;613:508–518.

[27] Verma Anurag, Huffman Jennifer E., Rodriguez Alex, et al. Diversity and Scale: Genetic Architecture of 2068 Traits in the VA Million Veteran Program *Science.* 2024;385:eadj1182.

[28] Zhou Wei, Kanai Masahiro, Wu Kuan-Han H., et al. Global Biobank Meta-analysis Initiative: Powering Genetic Discovery across Human Disease *Cell Genomics.* 2022;2:100192.

[29] Bycroft Clare, Freeman Colin, Petkova Desislava, et al. The UK Biobank Resource with Deep Phenotyping and Genomic Data *Nature.* 2018;562:203–209.

[30] Zheng Zhili, Liu Shouye, Sidorenko Julia, et al. Leveraging Functional Genomic Annotations and Genome Coverage to Improve Polygenic Prediction of Complex Traits within and between Ancestries *Nature Genetics.* 2024;56:767–777.

[31] Visscher Peter M., Yengo Loic, Cox Nancy J., Wray Naomi R.. Discovery and Implications of Polygenicity of Common Diseases *Science.* 2021;373:1468–1473.

[32] O'Connor Luke J., Schoech Armin P., Hormozdiari Farhad, Gazal Steven, Patterson Nick, Price Alkes L.. Extreme Polygenicity of Complex Traits Is Explained by Negative Selection *The American Journal of Human Genetics.* 2019;105:456–476.

[33] Zhang Yan, Qi Guanghao, Park Ju-Hyun, Chatterjee Nilanjan. Estimation of Complex Effect-Size Distributions Using Summary-Level Statistics from Genome-Wide Association Studies across 32 Complex Traits *Nature Genetics.* 2018;50:1318–1326.

[34] Zhang Yan Dora, Hurson Amber N., Zhang Haoyu, et al. Assessment of Polygenic Architecture and Risk Prediction Based on Common Variants across Fourteen Cancers *Nature Communications.* 2020;11.

[35] Fortea Juan, Pegueroles Jordi, Alcolea Daniel, et al. APOE4 Homozygosity Represents a Distinct Genetic Form of Alzheimer's Disease *Nature Medicine.* 2024;30:1284–1291.

[36] Lee Sang Hong, Wray Naomi R.. Novel Genetic Analysis for Case-Control Genome-Wide Association Studies: Quantification of Power and Genomic Prediction Accuracy ;8:e71494.

[37] Grotzinger Andrew D., Fuente Javier De La, Privé Florian, Nivard Michel G., Tucker-Drob Elliot M.. Pervasive Downward Bias in Estimates of Liability-Scale Heritability in Genome-wide Association Study Meta-analysis: A Simple Solution *Biological Psychiatry.* 2023;93:29–36.

[38] Tucker-Drob Elliot. 2.1 Calculating Sum of Effective Sample Size and Preparing GWAS Summary Statistics https://github.com/GenomicSEM/GenomicSEM/wiki/2.1-Calculating-Sum-of-Effective-Sample-Size-and-Preparing-GWAS-Summary-Statistics 2025.

[39] Thompson Deborah J., Wells Daniel, Selzam Saskia, et al. A Systematic Evaluation of the Performance and Properties of the UK Biobank Polygenic Risk Score (PRS) Release *PLOS ONE.* 2024;19:e0307270.

[40] Mars Nina, Lindbohm Joni V., Della Briotta Parolo Pietro, et al. Systematic Comparison of Family History and Polygenic Risk across 24 Common Diseases *The American Journal of Human Genetics.* 2022;109:2152–2162.

[41] Orchid Team . Alzheimer's Disease Whitepaper https://guides.orchidhealth.com/post/alzheimers-disease-whitepaper.

[42] Grotzinger Andrew D., Rhemtulla Mijke, de Vlaming Ronald, et al. Genomic Structural Equation Modelling Provides Insights into the Multivariate Genetic Architecture of Complex Traits *Nature Human Behaviour.* 2019;3:513–525.

[43] Willer Cristen J., Li Yun, Abecasis Gonçalo R.. METAL: Fast and Efficient Meta-Analysis of Genomewide Association Scans *Bioinformatics.* 2010;26:2190–2191.

[44] ReproGen Consortium , Psychiatric Genomics Consortium , Genetic Consortium for Anorexia Nervosa of the Wellcome Trust Case Control Consortium 3 , et al. An Atlas of Genetic Correlations across Human Diseases and Traits *Nature Genetics.* 2015;47:1236–1241.

[45] Mbatchou Joelle, Barnard Leland, Backman Joshua, et al. Computationally Efficient Whole-Genome Regression for Quantitative and Binary Traits *Nature Genetics.* 2021;53:1097–1103.

[46] Jiang Longda, Zheng Zhili, Qi Ting, et al. A Resource-Efficient Tool for Mixed Model Association Analysis of Large-Scale Data *Nature Genetics.* 2019;51:1749–1755.

[47] Institute National Cancer. SEER*Explorer: An Interactive Website for SEER Cancer Statistics. Updated September 26, 2024.

[48] Ferrari Alize J, Santomauro Damian Francesco, Aali Amirali, et al. Global Incidence, Prevalence, Years Lived with Disability (YLDs), Disability-Adjusted Life-Years (DALYs), and Healthy Life Expectancy (HALE) for 371 Diseases and Injuries in 204 Countries and Territories and 811 Subnational Locations, 1990–2021: A Systematic Analysis for the Global Burden of Disease Study 2021 *The Lancet.* 2024;403:2133–2161.

[49] Centers for Disease Control and Prevention . Data.CDC.gov website https://data.cdc.gov/. Accessed October 27, 2024.

[50] Lee Sang Hong, Goddard Michael E, Wray Naomi R, Visscher Peter M. A Better Coefficient of Determination for Genetic Profile Analysis *Genetic Epidemiology.* 2012;36:214–224.

[51] Manichaikul Ani, Mychaleckyj Josyf C., Rich Stephen S., Daly Kathy, Sale Michèle, Chen Wei-Min. Robust Relationship Inference in Genome-Wide Association Studies *Bioinformatics.* 2010;26:2867–2873.

[52] Orchid Health . Whitepapers https://guides.orchidhealth.com/category/whitepapers.

[53] Prediction Genomic. Risk Reduction Calculator https://www.lifeview.com/risk-reduction-calculator.

Supplementary Note: Assessment of Nucleus Genomics' polygenic score calibration and performance

In the course of conducting a comprehensive benchmark of polygenic embryo screening capabilities across commercial providers (see **Figure 3B**), we initially sought to include Nucleus Genomics (hereafter referred to as Nucleus), a direct-to-consumer genetic testing company providing disease risk predictions through physician reports, that recently expressed its intent to offer PGT-P. Given the absence of published performance validations by Nucleus, we performed an independent assessment using publicly available documentation and a set of five reports (three from European ancestry and two from non-European ancestry customers), made available to us with customer consent, from up to June 2025, in order to compare their performance to the other commercial providers.

Our evaluation showed considerable variability in the composition of the polygenic scores (PGS) provided by Nucleus. Nine of their disease PGSs appeared to be open-source models from the PGS catalog, almost all being five or more years old. Other disease predictions relied on variant sets notably smaller than typically required to adequately capture polygenic signals (**Supplementary Note Table 1**). For example, the polygenic score for attention-deficit hyperactivity disorder (ADHD) reportedly consisted of 12 variants, and a Parkinson's disease score contained 50 variants. These variant counts fall substantially below conventional benchmarks for using PGSs to predict traits with highly polygenic architectures. Further analysis suggests these smaller sets likely correspond to top-ranking genome-wide significant variants reported in previous genome-wide association studies (GWAS), an approach which typically yields limited predictive accuracy for highly polygenic diseases. Most of the scores seem furthermore to be identical to scores used by Nucleus' open source precursor Impute.me, implying that updates to their score set since the inception of the project as a for-profit business have been limited (see **Supplementary Table 8**). The only publicly documented update seems to have occurred on May 21st, 2025, when the company swapped a T2D PGS consisting of 171,249 variants (PGS Catalog ID: PGS000036) for another containing 1,259,754 variants (PGS Catalog ID: PGS002308).

Disease PGS	Number of variants	Median implied EUR liability R^2	UKBB validation EUR liability R^2 (SE)
Gastric cancer	6	0.1%	0.04% (.06)
ADHD	12	4.3%	0.007% (.30)
OCD	12	9.5%	0.004% (.05)
PCOS	14	8.1%	2.0% (.62)
Endometriosis	15	8.9%	0.011% (.10)
Anxiety disorders	20	8.3%	0.21% (.25)
Severe acne	20	8.1%	1.3% (.49)
Migraine	21	17.6%	0.65% (.40)
Hypertension	42	11.7%	0.65% (.46)
Parkinson's Disease	50	13.9%	0.73% (.30)
Asthma	152	10.7%	3.8% (.90)
Multiple sclerosis	283	10.2%	3.3% (.36)
Coronary artery disease	502	15.2%	6.2%* (1.3)

Supplementary Note Table 1: Nucleus disease PGSs with low numbers of variants with implied and validated liability R^2 values.
**Substantial overlap between the UKBB-containing PGS training sample and UKBB test set will have inflated the estimated liability R^2.*

To further assess the calibration and validity of their risk predictions, we converted reported absolute and relative risks into implied liability-scale variance explained (liability R^2) via standard liability-threshold transformations (**Methods**). Across the five customer reports, we noted substantial variability and inconsistencies in the implied predictive performance, with, for example, schizophrenia having implied liability R^2 ranging from 0% to 5% (**Supplementary Table 9**). We also noted several examples where the liability R^2 exceeded realistic expectations given the number of variants included in the PGS. For instance, the hypertension PGS, which included only 42 variants, had an implied median liability R^2 values exceeding 10% (**Supplementary Table 9**). We were unable to identify public documentation provided by Nucleus that would explain these results. Available reports included statements qualifying the predictive performance of PGS models ("*Science's current ability to use common DNA variants to predict a person's risk of developing [disease] is limited [or 'extremely limited' for some diseases].*") for gastric cancer, depression, ovarian cancer, osteoarthritis, bipolar disorder and colorectal cancer.

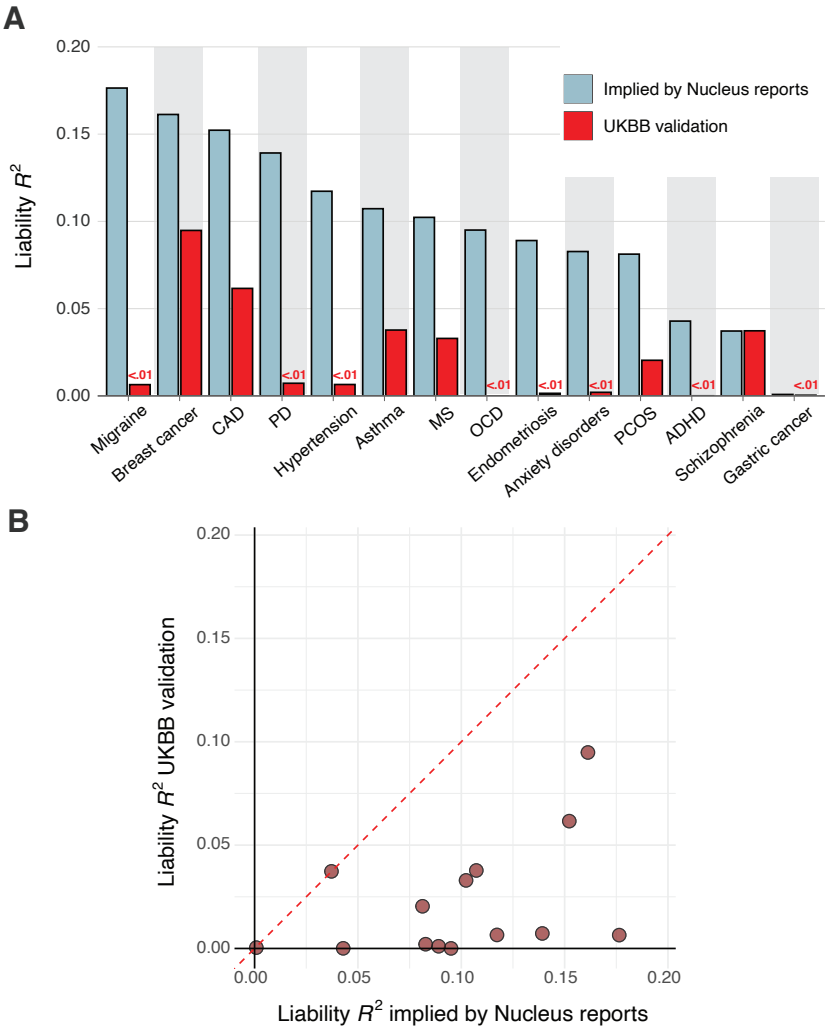

Supplementary Note Figure 1: Comparison of Nucleus-implied median liability R^2 (blue) with UKBB validation for the best-matched score (red). (A) Bar chart of median values. (B) Scatterplot of median Nucleus values versus UKBB values; the dashed red line marks the identity $y = x$.

We compared Nucleus' reported risk predictions against our independent UKBB validation for PGS models we could reliably match to their likely scores (see **Supplementary Table 8** for the best-matched PGS model source). For nearly all diseases, the median implied performance derived from Nucleus Genomics reports collected from customers of European ancestry was consistently (and often substantially) higher than our independently validated performance estimates (**Supplementary Note Figure 1**). Notably, for two PGSs where we found literature-based performance estimates, the estimates from our own validation in UKBB were highly concordant (**Supplementary Note Table 2**). This concordance suggests that our independent validation was consistent with externally conducted validations. Overall, we found that the PGSs likely used by Nucleus display substantially lower predictive performance than that implied by their customer reports.

Disease PGS	UKBB validation	Reported in literature
Breast cancer	0.095 (.069, .12)	0.093 (0.087, 0.10)
Schizophrenia	0.037 (.027, .050)	0.035 (0.015, 0.062)

Supplementary Note Table 2: Comparison of PGS liability R^2 and 95% confidence intervals estimated in our UKBB validation versus those reported in the literature (see **Supplementary Table 8** for more details).

We also performed a preliminary analysis of Nucleus' advertised risk reductions when applying their PGS models in PGT-P. To this end, we extracted data from Nucleus' online risk reduction calculator[1], which, for nine diseases, displays the disease's population prevalence alongside the risk reduced when selecting the embryo with the lowest predicted risk among two to five embryos. The interpretation of these reductions is complicated by the use of prevalences pertaining to various narrow subsets of the population. For example, the reported coronary artery disease (CAD) risks were "calculated for males with one major risk factor," where major risk factors included smoking, having diabetes, blood pressure (160/100 or above), and high cholesterol (240 and above). The source (Table 3 of Lloyd-Jones et al.[2]) matches that cited in Nucleus' physician reports. For other traits, the population prevalences were uncited but identically matched those in the respective physician reports.

This raises the question of whether the reported embryo-level risk reductions apply exclusively to embryos whose future cardiovascular profiles match the described high-risk subset (e.g., males with at least one major risk factor). If so, the interpretation is unclear, as embryo phenotypes cannot be known in advance—and many risk factors themselves partially reflect underlying genetic liability for CAD. If Nucleus derived risk reductions using such narrowly defined subgroups, the reported reductions would not reflect expected risk in a general embryo population. Moreover, if these subsets were chosen based on convenience (e.g., the first figure from the CAD PGS source publication), it raises further questions about methodological rigor.

We collated these prevalences, risk reductions, and Nucleus' cited disease heritabilities in order to simulate the risk reductions permitted by a given PGS model liability R^2 using the same approach described above ("*Simulations of expected gains from use of PGS models in PGT-P*"). We conducted a limited grid search up to $\pm 10\%$ on either side of the median liability R^2 previously inferred from physician reports, with step sizes of 0.5%, selecting the three estimates best minimizing the sum of reported minus simulated risk reductions across the displayed embryo batch sizes (**Supplementary Table 10**). Although broadly informative, this procedure did not permit confident mapping of embryo-level risk reductions to specific PGS models reconstructed from physician reports.

Nonetheless, in several instances the implied liability R^2 estimates from embryo selection fell within the range inferred from adult reports. For instance, embryo versus adult median European liability R^2 values were 10–11% versus 9.2% for age-related macular degeneration, and 8–9% versus 8.1% for PCOS (**Supplementary Table 10**). However, substantial discrepancies emerged for traits such as schizophrenia, rheumatoid arthritis, and endometriosis, where inferred embryo-selection liability R^2 values differed considerably from those derived from adult reports. Though such comparisons rely on untestable assumptions concerning Nucleus' methodology, either possibility—namely that the same questionable PGS models are used in both adult and embryo products or that an unknown set is employed solely for the latter—erodes confidence in

the accuracy and reliability of Nucleus' reported risk reductions. This uncertainty underscores the critical need for calibrated risk estimates, transparent reporting of model validation, and full disclosure of methodology and its assumptions.

Finally, given the above evidence in favor of substantially inflated predictive performances of Nucleus' PGS models, we sought to informally evaluate hypotheses that might explain the magnitude and breadth of the likely errors. One possible explanation is suggested by the similarity of the implied liability R^2 values to estimates of loosely related parameters in the source GWASs used for PGS training. For example, the median liability R^2 of 17.6% implied by Nucleus' migraine risk predictions for European customers is closest to a measure of the *SNP heritability* of 14.6% cited in Supplementary Figure 6 of Gormley et al.[3], the PGS's corresponding 2016 migraine GWAS. Crucially, this parameter indexes the proportion of liability variance explained by the additive effects of *all* common causal variants[4] rather than just those whose GWAS effects are imprecisely estimated and included in a 21-SNP score. Likewise, Nucleus' median implied R^2 of 4.3% for ADHD better matches the headline PGS $R^2 \sim 5.5\%$ returned from the leave-one-cohort-out PRS validation in Demontis et al.[5]; however, this result relates to PGS built with liberal pruning and thresholding, which therefore contain hundreds of thousands of SNPs in addition to the 12 included in Nucleus' ADHD model. A similar explanation may also hold for diseases of greater consequence such as breast cancer, for which an implied liability R^2 of 16.1% better matches the sum of winner's curse-unadjusted variance explained by all GWAS susceptibility loci (18%) in Michailidou et al.[6] than our concordant literature and UKBB validation estimates of liability $R^2 \sim 9.5\%$ (**Supplementary Note Table 2**). The same is true of the implied liability R^2 versus SNP heritability for asthma (10.7% vs. 10.6% for adult-onset asthma[7]), insomnia (10.3% vs. 9–11%, see the "SNP heritability" section of Hammerschlag et al.[8]) and hypertension (11.7% vs. 10.7%[9]), perhaps among others.

Given these cumulative concerns and lack of published external validation, we concluded that inclusion of Nucleus' scores in our primary benchmarking comparison would not yield a reliable or meaningful addition to our analysis.

Supplementary Tables

Trait	UK Biobank phenotype code
Alanine aminotransferase	30620
Albumin	30600
Alkaline phosphatase	30610
Ankle spacing width	3143
Apolipoprotein A	30630
Aspartate aminotransferase	30650
Blood urea nitrogen	30670
Calcium	30680
Coronary artery disease	131298, 131300, 131302, 131304, 131306, 41272 (OPCS4 codes K40, K41, K45, K49, K502, K75), 20002 (self report code 1075), 6150
Corpuscular volume	30040
Creatinine	30700
Cystatin C	30720
ECG PQ interval	22330
ECG QRS duration	12340
ECG QTC interval	22332
Eosinophil percentage	30210
Erythrocyte count	30010
Erythrocyte width	30070
Estimated glomerular filtration rate (creatinine-based)	30700
Gamma glutamyl transferase	30730
Glucose	30740
Grip strength	46, 47
Heel ultrasound attenuation	3144
Hematocrit percentage	30030
IGF-1	30770
Insomnia	130920, 20002 (self-report code 1616)
Monocyte percentage	30190

Trait	UK Biobank phenotype code
Phosphate	30810
Platelet distribution width	30110
Refractive error (avMSE)	20261
Reticulocyte fraction	30280
Sex hormone-binding globulin	30830
Sodium	30530
Speed of sound through heel	3146
Suicide attempt	20002 (self-report code 1290), 20483, 29116
Testosterone (female-only)	30850
Testosterone (male-only)	30850
Thrombocyte volume	30100
Triglycerides	30870
Urate	30880
Ventricular rate	12336
Vitamin D	30890
Water mass of whole body	23102
Vitiligo	131802, 20002 (self-report code 1661)
Systemic lupus erythematosus	131894, 20002 (self-report code 1381)
Thoracic aortic aneurysm	131382
Testicular cancer	40006 (ICD10 cancer code C62), 20001 (self-report code 1045)
Gout	131858, 20002 (self-report code 1466)
Attention-Deficit/Hyperactivity Disorder	130976, 20544, 29000
Crohn's disease	131626, 20002 (self-report code 1462)
Multiple sclerosis	131042, 20002 (self-report code 1261)
Psoriasis	131742, 20002 (self-report code 1453)

Trait	UK Biobank phenotype code
Ulcerative colitis	131628, 20002 (self-report code 1463)
Parkinson's disease	131022, 20002 (self-report code 1262)
Atopic dermatitis	131720
Inflammatory bowel disease	131626, 131628, 20002 (self-report codes 1462, 1463)
Kidney cancer	40006 (ICD10 cancer code C64), 20001 (self-report code 1042)
Osteoporosis	131962, 131964, 131966, 20002 (self-report code 1309)
Melanoma	40006 (ICD10 cancer code C43), 20001 (self-report code 1059)
Acne	131790, 20002 (self-report code 1548)
Alzheimer's disease	131036, 130836, 20002 (self-report code 1263)
Age-related macular degeneration	131182, 20002 (self-report code 1528)
Glaucoma	131186, 6148, 6119, 20002 (self-report code 1277),
Rheumatoid arthritis	131848, 131850, 120001, 20002 (self-report code 1464)
Bipolar disorder	130892, 20126, 20544, 20002 (self-report code 1291)
Chronic obstructive pulmonary disease	131486, 131488, 131490, 131492, 22130, 22170, 22128, 22168, 20002 (self-report codes 1112, 1113)
Basal cell carcinoma	40006 (ICD10 cancer code C44), 20002 (self-report code 1061)
Schizophrenia	130874, 20544, 29000, 20002 (self-report code 1289)
Birth weight	20022
Colorectal cancer	40006 (ICD10 cancer codes C18-20), 20001 (self-report codes 1020, 1022, 1023)

Trait	UK Biobank phenotype code
Migraine	131052, 120016, 20002 (self-report code 1265)
Prostate cancer	40006 (ICD10 cancer code C61), 20001 (self-report code 1044)
Chronic kidney disease	132032 (only ICD10 codes N183-5), 30700 (eGFR $<$ mL/min), 20002 (self-report code 1192)
Diverticular disease	131636, 20002 (self-report code 1458)
Stroke	131362, 131366, 6150, 20002 (self-report codes 1081, 1583)
Venous thromboembolism	131308, 131396, 131400, 41272 (OPCS4 codes O871, O882), 20002 (self-report codes 1093, 1094, 1068)
Hearing loss	131258, 2247, 2257
Sleep duration	1160
Breast cancer	40006 (ICD10 cancer code C50), 20001 (self-report code 1002)
Chronotype	1180
Atrial fibrillation	131350, 41272 (OPCS4 codes K57, K62), 20002 (self-report codes 1471, 1483)
Hypertension	131286, 20002 (self-report codes 1065, 1072)
Asthma	131494, 131496, 6152, 22167, 20002 (self-report code 1111)
Type 2 diabetes	130708, 20002 (self-report code 1223)
Restless legs syndrome	131032
Body mass index	21001

Supplementary Table 1: Phenotype definitions used for disease and the traits used in UK Biobank for validation and relative PGS performance attenuation in diverse ancestries.

Category	Disease	Liability R^2 (95% CI)
Cancer	Prostate cancer	19.0% (15.6, 22.9)
	Breast cancer	14.3% (10.9, 17.5)
	Basal cell carcinoma	11.9% (8.9, 15.2)
	Testicular cancer	7.6% (6.4, 9.3)
	Melanoma	7.4% (5.4, 9.5)
Metabolic and cardiovascular	Type 2 diabetes	20.7% (16.8, 24.8)
	Hypertension	15.7% (12.0, 19.3)
	Gout	10.4% (7.9, 13.2)
	Venous thromboembolism	5.7% (3.7, 8.0)
Neurological	Alzheimer's disease	16.1% (12.3, 20.5)
	Multiple sclerosis	7.0% (6.0, 8.0)
Inflammatory and autoimmune	Psoriasis	11.6% (9.1, 14.7)
	Atopic dermatitis	10.9% (6.6, 16.0)
	Vitiligo	9.9% (7.9, 12.1)
	Inflammatory bowel disease	7.5% (5.7, 9.4)
Other	Glaucoma	8.2% (6.0, 10.8)
	Osteoporosis	7.1% (4.5, 10.1)

Supplementary Table 2: Liability R^2 estimated between families in the UK Biobank for 17 newly developed disease PGS.

Disease	Lifetime risk (EUR) M	Lifetime risk (EUR) F	Source
Vitiligo	0.45%	0.46%	Howitz et al., 1977 [10]
Testicular cancer	0.49%		SEER, 2024 [11]
Gout	11.00%	3.10%	Dehlin et al., 2020 [12]
Multiple sclerosis	0.19%	0.54%	Hittle et al. 2023 [13]
Psoriasis	2.90%	2.90%	Pezzolo et al., 2019 [14]
Atopic dermatitis	12.00%	12.00%	Hadi et al., 2021 [15]
Inflammatory bowel disease	1.69%	1.85%	Forss et al. 2022 [16]
Osteoporosis	22.00%	46.00%	Kanis et al., 2000 [17]
Melanoma	3.47%	2.48%	SEER, 2024 [11]
Alzheimer's disease	8.80%	13.40%	Lobo et al., 2011 [18]
Glaucoma	5.53%	8.51%	NEI, 2024 [19]
Venous thromboembolism	7.70%	8.40%	Bell et al., 2016 [20]
Prostate cancer	12.57%		SEER, 2024 [11]
Basal cell carcinoma	21.00%	18.00%	Flohil et al., 2013 [21]
Breast cancer		13.87%	SEER, 2024 [11]
Hypertension	45.40%	48.30%	FinnGen, 2024 [22]
Type 2 diabetes	21.40%	18.40%	Narayan et al., 2007 [23]

Supplementary Table 3: Lifetime risk estimates and their corresponding sources for European ancestry individuals for males (M) and females (F).

Ancestry	Type 2 diabetes lifetime risk M	Type 2 diabetes lifetime risk F
SAS	26.40%	24.19%
EAS	27.59%	23.72%
AFR	26.35%	28.61%

Supplementary Table 4: Lifetime risk estimates for type 2 diabetes by individual ancestries as reported in Narayan et al. (2007)[23] for males (M) and females (F).

Conversion	Expression or term	Definition
Odds-ratio per 1 SD of PGS (OR) $\rightarrow$ Cohen's d	p	sample prevalence
	$d\colon \mathrm{OR} = \exp\left(d\sqrt{1+d^2p(1-p)}\right)$	(solved numerically for d)
Area under ROC curve (AUC) $\rightarrow$ Cohen's d	$z = \Phi^{-1}(\mathrm{AUC})$	liability z-score
	$d = \sqrt{2}\,z$	standardized mean difference between PGS of cases and controls
Cohen's $d \rightarrow$ observed-scale R_o^2	$R_o^2 = \dfrac{d^2\,p\,(1-p)}{1+d^2\,p\,(1-p)}$	observed-scale R_o^2
Observed-scale R_o^2 $\rightarrow$ liability-scale R_l^2	$t = \Phi^{-1}(1-k)$	case threshold for lifetime risk k
	$z = \varphi(t)$	standard-normal PDF at t
	$i = \dfrac{z}{k}$	mean liability of cases
	$C = \dfrac{[k(1-k)]^2}{z^2\,p\,(1-p)}$	variance scaling factor
	$\theta = i\left(\frac{p-k}{1-k}\right)\left(i\left(\frac{p-k}{1-k}\right) - t\right)$	ascertainment adjustment
	$R_l^2 = \dfrac{C\,R_o^2}{1+C\,\theta R_o^2}$	liability-scale R_l^2

Supplementary Table 5: Equations used to convert comparison validations reported in odds ratios or AUC to liability R^2.

Disease *(Number of proband cases in parentheses)*	**Estimand**	$\hat{\beta}$, $\hat{r}$ **or** $\hat{\beta}_{direct}/\hat{\beta}_{pop}$	**SE**	p
Alzheimer's disease (465)	Population effect	0.221	0.022	1.5×10^{-24}
	Direct effect	0.218	0.036	1.8×10^{-9}
	Average non-transmitted coefficient	0.003	0.029	0.907
	Direct/population effect ratio	0.970	0.128	0.813
	Spousal PGS correlation	0.011	0.008	0.203
Atopic dermatitis (22)	Population effect	0.267	0.064	3.5×10^{-5}
	Direct effect	0.241	0.112	0.031
	Average non-transmitted coefficient	0.026	0.091	0.772
	Direct/population effect ratio	0.912	0.433	0.838
	Spousal PGS correlation	0.008	0.009	0.323
Basal cell carcinoma (2395)	Population effect	0.260	0.011	1.1×10^{-121}
	Direct effect	0.281	0.019	5.8×10^{-49}
	Average non-transmitted coefficient	−0.020	0.016	0.191
	Direct/population effect ratio	1.070	0.060	0.212
	Spousal PGS correlation	0.008	0.009	0.359
Breast cancer (1863)	Population effect	0.280	0.013	6.7×10^{-105}
	Direct effect	0.258	0.022	2.6×10^{-32}
	Average non-transmitted coefficient	0.022	0.018	0.212
	Direct/population effect ratio	0.923	0.064	0.227
	Spousal PGS correlation	−0.023	0.009	0.008
Glaucoma (1257)	Population effect	0.252	0.014	5.6×10^{-73}
	Direct effect	0.265	0.024	1.7×10^{-28}
	Average non-transmitted coefficient	−0.014	0.020	0.483
	Direct/population effect ratio	1.050	0.078	0.509
	Spousal PGS correlation	−0.009	0.009	0.285
Gout (1154)	Population effect	0.270	0.014	5.2×10^{-80}
	Direct effect	0.268	0.025	3.7×10^{-26}
	Average non-transmitted coefficient	0.003	0.021	0.895
	Direct/population effect ratio	0.989	0.076	0.880
	Spousal PGS correlation	0.012	0.008	0.140
Hypertension (15096)	Population effect	0.351	0.007	$< 10^{-300}$
	Direct effect	0.334	0.012	7.4×10^{-164}
	Average non-transmitted coefficient	0.017	0.010	0.087
	Direct/population effect ratio	0.951	0.028	0.078
	Spousal PGS correlation	0.003	0.009	0.733
Inflammatory bowel disease (705)	Population effect	0.266	0.017	7.1×10^{-58}
	Direct effect	0.252	0.028	8.6×10^{-19}

Continued on next page

Supplementary Table 6 (continued)

Disease *(Number of proband cases in parentheses)*	**Estimand**	$\hat{\beta}$, $\hat{r}$ **or** $\hat{\beta}_{direct}/\hat{\beta}_{pop}$	**SE**	p
	Average non-transmitted coefficient	0.014	0.023	0.543
	Direct/population effect ratio	0.945	0.090	0.541
	Spousal PGS correlation	0.014	0.008	0.096
Melanoma (385)	Population effect	0.162	0.019	1.0×10^{-16}
	Direct effect	0.181	0.034	1.5×10^{-7}
	Average non-transmitted coefficient	−0.019	0.028	0.501
	Direct/population effect ratio	1.120	0.184	0.520
	Spousal PGS correlation	0.012	0.008	0.167
Multiple sclerosis (237)	Population effect	0.299	0.024	1.8×10^{-35}
	Direct effect	0.287	0.042	9.8×10^{-12}
	Average non-transmitted coefficient	0.012	0.035	0.732
	Direct/population effect ratio	0.955	0.117	0.702
	Spousal PGS correlation	0.004	0.009	0.681
Osteoporosis (2120)	Population effect	0.180	0.012	4.6×10^{-53}
	Direct effect	0.139	0.020	8.3×10^{-12}
	Average non-transmitted coefficient	0.041	0.017	0.015
	Direct/population effect ratio	0.786	0.091	0.019
	Spousal PGS correlation	0.004	0.009	0.646
Prostate cancer (1157)	Population effect	0.342	0.017	2.0×10^{-87}
	Direct effect	0.359	0.029	1.1×10^{-34}
	Average non-transmitted coefficient	−0.018	0.024	0.462
	Direct/population effect ratio	1.050	0.069	0.470
	Spousal PGS correlation	−0.006	0.009	0.464
Psoriasis (886)	Population effect	0.277	0.015	4.5×10^{-76}
	Direct effect	0.303	0.026	5.5×10^{-31}
	Average non-transmitted coefficient	−0.027	0.021	0.215
	Direct/population effect ratio	1.090	0.080	0.267
	Spousal PGS correlation	0.006	0.009	0.495
Testicular cancer (69)	Population effect	0.273	0.044	8.4×10^{-10}
	Direct effect	0.265	0.075	4.5×10^{-4}
	Average non-transmitted coefficient	0.008	0.060	0.893
	Direct/population effect ratio	1.020	0.229	0.948
	Spousal PGS correlation	0.006	0.009	0.480
Type 2 diabetes (3027)	Population effect	0.380	0.011	3.4×10^{-262}
	Direct effect	0.384	0.018	9.0×10^{-96}
	Average non-transmitted coefficient	−0.003	0.015	0.829
	Direct/population effect ratio	1.010	0.039	0.797

Continued on next page

Supplementary Table 6 (continued)

Disease *(Number of proband cases in parentheses)*	**Estimand**	$\hat{\beta}$, $\hat{r}$ **or** $\hat{\beta}_{direct}/\hat{\beta}_{pop}$	**SE**	p
	Spousal PGS correlation	0.009	0.009	0.290
Venous thromboembolism (2051)	Population effect	0.201	0.011	1.1×10^{-70}
	Direct effect	0.199	0.019	6.5×10^{-25}
	Average non-transmitted coefficient	0.002	0.016	0.909
	Direct/population effect ratio	0.993	0.076	0.924
	Spousal PGS correlation	0.002	0.009	0.851
Vitiligo (41)	Population effect	0.260	0.051	3.1×10^{-7}
	Direct effect	0.366	0.091	5.5×10^{-5}
	Average non-transmitted coefficient	−0.100	0.070	0.154
	Direct/population effect ratio	1.370	0.312	0.239
	Spousal PGS correlation	0.085	0.008	3.1×10^{-27}

Supplementary Table 6: Within-family model estimates. "Direct effect" and "Average non-transmitted coefficient" refer to the estimated coefficients on a proband PGS term and combined maternal + paternal PGS term in the within-family specification, respectively. "Direct/population effect ratio" refers to the ratio of direct to population effects derived from a within-family model fitting maternal and paternal PGS terms separately.

Disease	Orchid sample prevalence	Genomic Prediction sample prevalence
Alzheimer's	omitted	∼1.2%
Basal cell carcinoma	not validated	∼1.4%
Breast cancer	8.0%	∼4.7%
Type 2 diabetes	7.5%	∼6.4%
Gout	not validated	∼2%
Hypertension	not validated	∼32%
Inflammatory bowel disease	1.5%	∼1.5%
Melanoma	not validated	∼0.9%
Prostate cancer	7.4%	∼2.1%
Testicular cancer	not validated	∼0.4%

Supplementary Table 7: Sample prevalences used to convert PGS AUC reported by commercial PGT-P providers to liability R^2 shown in Figure 3. Values for Genomic Prediction were approximated using the available information in the supplement to Widen et al. [24] and on Genomic Prediction's risk reduction calculator webpage[25]. Values for Orchid were found in their online whitepapers[26].

Trait	Ver.	#SNPs	Sources used to identify PGS *(+Impute.me)*	Public PGS weights link	PGS weights type	Nucleus prevalence	Literature R^2 (95% CI)	Literature R^2 derivation
Gastric cancer	v1	6	physician reports + rsIDs + GWAS Catalog	https://www.ebi.ac.uk/gwas/studies/GCST006707	GWAS lead SNP effects			
ADHD	v1	12	physician reports + rsIDs + GWAS sumstats	https://figshare.com/articles/dataset/adhd2019/14671965?file=28169253	GWAS lead SNP effects			
OCD	v1	12	physician reports + rsIDs + GWAS Catalog	https://www.ebi.ac.uk/gwas/studies/GCST003434	GWAS lead SNP effects			
PCOS	v1	14	physician reports + rsIDs + GWAS Catalog	https://www.ebi.ac.uk/gwas/studies/GCST007089	GWAS lead SNP effects			
Endometriosis	v1	15	physician reports + rsIDs + GWAS Catalog	https://www.ebi.ac.uk/gwas/studies/GCST004549	GWAS lead SNP effects			
Age-related macular degeneration	v1	16	physician reports + rsIDs + GWAS Catalog	https://www.ebi.ac.uk/gwas/studies/GCST001884	GWAS lead SNP effects			
Restless legs syndrome	v1	18	physician reports + rsIDs + GWAS Catalog	https://www.ebi.ac.uk/gwas/studies/GCST005042	GWAS lead SNP effects			
Anxiety disorders	v1	20	physician reports + GWAS Catalog	https://www.ebi.ac.uk/gwas/studies/GCST007710	GWAS lead SNP effects			
Severe acne	v1	20	physician reports + rsIDs + GWAS Catalog	https://www.ebi.ac.uk/gwas/studies/GCST007234	GWAS lead SNP effects			
Migraine	v1	21	physician reports + rsIDs + GWAS Catalog	https://www.ebi.ac.uk/gwas/studies/GCST003720	GWAS lead SNP effects			
Celiac disease	v1	23	physician reports + rsIDs + GWAS Catalog	https://www.ebi.ac.uk/gwas/studies/GCST000612	GWAS lead SNP effects			
Osteoarthritis	v1	30	physician reports + rsIDs + GWAS Catalog	https://www.ebi.ac.uk/gwas/studies/GCST007093	GWAS lead SNP effects			
Alzheimer's disease	v1	33	physician report + PGS Catalog	https://www.pgscatalog.org/score/PGS000026	PGS Catalog weights			
Chronic pain	v1	37	physician reports + rsIDs + GWAS Catalog	https://www.ebi.ac.uk/gwas/studies/GCST008512	GWAS lead SNP effects			
Hypertension	v1	42	physician reports + rsIDs + GWAS Catalog	https://www.ebi.ac.uk/gwas/studies/GCST007707	GWAS lead SNP effects			
Parkinson's disease	v1	50	physician reports + rsIDs + GWAS Catalog	https://www.ebi.ac.uk/gwas/studies/GCST004902	GWAS lead SNP effects			
Male pattern baldness	v1	51	physician reports + rsIDs + GWAS sumstats	https://doi.org/10.1038/s41467-017-01490-8	GWAS lead SNP effects			
Seasonal allergies	v1	80	physician reports + rsIDs + GWAS Catalog	https://www.ebi.ac.uk/gwas/studies/GCST009716	GWAS lead SNP effects			
Asthma	v1	152	physician reports + rsIDs + GWAS Catalog	https://www.ebi.ac.uk/gwas/studies/GCST007798	GWAS lead SNP effects			
Multiple sclerosis	v1	283	physician reports + rsIDs + GWAS Catalog	https://www.ebi.ac.uk/gwas/studies/GCST009597	GWAS lead SNP effects			
Longevity	v1	332	physician reports + rsIDs + GWAS Catalog	https://www.pgscatalog.org/score/PGS000906	GWAS lead SNP effects			
Coronary artery disease	v1	502	physician reports + rsIDs + GWAS sumstats	https://data.mendeley.com/datasets/gbbsrpx6bs/1	GWAS lead SNP effects			

Continued on next page

Continued from previous page

Trait	Ver.	#SNPs	Sources used to identify PGS *(+Impute.me)*	Public PGS weights link	PGS weights type	Nucleus prevalence	Literature R^2 (95% CI)	Literature R^2 derivation
Type 2 diabetes	v1	171 249	physician reports + Impute.me `study_list` (LF 2020-12-28)	https://www.pgscatalog.org/score/PGS000036	PGS Catalog weights	33 %	10.4 % (9.6, 11.1)	Converted from OR (PPM021436)
Height	v1	416 877	physician reports + Impute.me `study_list` (LF 2020-12-28)	http://lianglab.rc.fas.harvard.edu/CTPR/CTPR_beta_coefficients.tar.gz (`ldpred`)	Public PGS weights			
Body mass index	v1	503 330	physician reports + Impute.me `study_list` (LF 2019-03-18)	(internally trained by Impute.me)	Internal weights			
Bipolar disorder	v1	554 976	physician reports + Impute.me `study_list` (LF 2019-03-18)	(internally trained by Impute.me)	Internal weights			
Intelligence	v1	558 032	physician reports + Impute.me `study_list` (LF 2019-03-18)	(internally trained by Impute.me)	Internal weights			
Depression	v1	558 415	physician reports + Impute.me `study_list` (LF 2019-03-18)	(internally trained by Impute.me)	Internal weights			
Alcohol dependence	v1	558 693	physician reports + Impute.me `study_list` (LF 2019-03-18)	(internally trained by Impute.me)	Internal weights			
Insomnia	v1	558 823	physician reports + Impute.me `study_list` (LF 2019-10-30)	(internally trained by Impute.me)	Internal weights			
Schizophrenia	v1	833 502	physician reports + Impute.me `study_list` (LF 2020-12-28)	https://www.pgscatalog.org/score/PGS000136	PGS Catalog weights	0.6 %	3.5 % (1.5, 6.2)	Converted from OR (PPM000416)
Breast cancer	v1	1 079 067	physician reports + Impute.me `study_list` (LF 2020-12-28)	https://www.pgscatalog.org/score/PGS000335	PGS Catalog weights	13 %	9.3 % (8.7, 10.0)	Converted from OR (PPM000903)
Male breast cancer	v1	1 079 067	physician reports + Impute.me `study_list` (LF 2020-12-28)	https://www.pgscatalog.org/score/PGS000335	PGS Catalog weights			
Prostate cancer	v1	1 111 494	physician reports + Impute.me `study_list` (LF 2020-12-28)	https://www.pgscatalog.org/score/PGS000566	PGS Catalog weights	8 %	2.6 % (1.7, 3.8)	Converted from OR (PPM001251)
Ovarian cancer	v1	1 115 189	physician reports + Impute.me `study_list` (LF 2020-12-28)	https://www.pgscatalog.org/score/PGS000546	PGS Catalog weights	1 %	0.2 % (0.03, 0.6)	Converted from OR (PPM001231)
Colorectal cancer	v1	1 119 238	physician reports + Impute.me `study_list` (LF 2020-12-28)	https://www.pgscatalog.org/score/PGS000373	PGS Catalog weights	4 %	0.6 % (0.1, 1.3)	Converted from OR (PPM001058)
Type 2 diabetes	v2	1 259 754	physician report + PGS Catalog (updated 2025-05-21)	https://www.pgscatalog.org/score/PGS002308	PGS Catalog weights	33 %	14.7 % (13.7, 15.8)	Converted from OR (PPM013064)

Supplementary Table 8: Nucleus PGS models reconstructed by matching variant counts shown on physician reports with external sources of SNP rsIDs and weights. "Impute.me `study_list` sheet" refers to `2021-02-11_study_list.xlsx` on the Impute.me GitHub repository.[27]

Disease	N	Minimum	q25	Median	Median (EUR reports only)	Mean	q75	Maximum	SD
Breast cancer	1	0.1613	0.1613	0.1613	0.1613	0.1613	0.1613	0.1613	NA
Migraine	21	0.0004	0.0741	0.1525	0.1764	0.1252	0.1949	0.2181	0.0768
Coronary artery disease	13	0.0226	0.0835	0.1187	0.1522	0.1184	0.1570	0.1734	0.0462
Type 2 diabetes	21	0.0374	0.0850	0.1220	0.1306	0.1143	0.1367	0.2718	0.0498
Chronic pain	16	0.0489	0.0854	0.1160	0.1319	0.1132	0.1420	0.1592	0.0359
Parkinson's disease	5	0.0170	0.0787	0.1311	0.1392	0.1068	0.1392	0.1681	0.0597
Restless legs syndrome	5	0.0616	0.0806	0.0942	0.0942	0.0942	0.1172	0.1174	0.0241
Asthma	12	0.0468	0.0802	0.0993	0.1073	0.0937	0.1144	0.1341	0.0294
Insomnia	16	0.0461	0.0776	0.0989	0.1034	0.0923	0.1131	0.1280	0.0272
Endometriosis	1	0.0890	0.0890	0.0890	0.0890	0.0890	0.0890	0.0890	NA
Hypertension	17	0.0038	0.0617	0.1065	0.1173	0.0886	0.1268	0.1407	0.0469
Alcohol dependence	8	0.0004	0.0533	0.0899	0.1063	0.0839	0.1153	0.1514	0.0478
PCOS	3	0.0803	0.0808	0.0812	0.0812	0.0830	0.0843	0.0874	0.0038
Male breast cancer	2	0.0693	0.0748	0.0803	0.0803	0.0803	0.0858	0.0913	0.0155
Multiple sclerosis	5	0.0128	0.0437	0.1003	0.1023	0.0777	0.1023	0.1294	0.0479
OCD	4	0.0486	0.0517	0.0739	0.0950	0.0776	0.0998	0.1142	0.0322
Age-related macular degeneration	20	0.0019	0.0404	0.0840	0.0925	0.0767	0.1118	0.1479	0.0463
Prostate cancer	13	0.0220	0.0442	0.0697	0.0744	0.0746	0.0898	0.2158	0.0494
Anxiety disorders	16	0.0332	0.0412	0.0753	0.0827	0.0698	0.0852	0.1036	0.0246
Rheumatoid arthritis	20	0.0000	0.0495	0.0773	0.0782	0.0676	0.0895	0.1291	0.0358
Severe acne	3	0.0145	0.0237	0.0328	0.0812	0.0595	0.0820	0.1311	0.0627
ADHD	13	0.0181	0.0286	0.0405	0.0429	0.0408	0.0509	0.0716	0.0149
Schizophrenia	24	0.0000	0.0241	0.0312	0.0372	0.0317	0.0410	0.0499	0.0137
Colorectal cancer	5	0.0124	0.0253	0.0254	0.0270	0.0236	0.0270	0.0280	0.0064
Osteoarthritis	12	0.0090	0.0158	0.0236	0.0312	0.0236	0.0321	0.0344	0.0095
Bipolar disorder	5	0.0072	0.0110	0.0111	0.0123	0.0108	0.0123	0.0124	0.0021
Depression	4	0.0024	0.0040	0.0051	0.0057	0.0107	0.0118	0.0301	0.0130
Ovarian cancer	1	0.0010	0.0010	0.0010	0.0011	0.0010	0.0010	0.0010	NA
Gastric cancer	5	0.0000	0.0000	0.0008	0.0009	0.0010	0.0014	0.0026	0.0011

Supplementary Table 9: Summary statistics of liability R^2 per trait, including the median from European-ancestry reports.

Disease	Prevalence used in embryo risk reduction calculator	Nucleus heritability *if not provided, cited from the literature*	Median EUR liability R^2 inferred from adult physician's reports *(Supplementary Table 8)*	Top selected liability R^2 from embryo risk reduction simulations
Type 2 diabetes	19.8%	72%	13.1%	9–10%
Coronary artery disease	37.6%	50%	15.2%	10–11%
Restless legs syndrome	9.0%	54%	9.4%	11–12%
Endometriosis	11%[28]	47%[28]	8.9%	6–7%
Age-related macular degeneration	17.7%	59%	9.2%	10–11%
PCOS	9.6%	72%[29]	8.1%	8–9%
Rheumatoid arthritis	1.7%	58%	7.8%	15–16%
Prostate cancer	8.2%	58%	7.4%	9.5–10.5%
Schizophrenia	1.1%	83%	3.7%	7–8%

Supplementary Table 10: Liability R^2 inferred from Nucleus' adult physician's reports and embryo risk-reduction calculator[1]. Prevalences and heritabilities were scraped from Nucleus materials for input to risk-reduction simulations unless otherwise noted.

References

[1] Nucleus Genomics . The Science behind Nucleus Embryo *Nucleus.* 2025. Accessed July 17, 2025.

[2] Lloyd-Jones Donald M., Leip Eric P., Larson Martin G., et al. Prediction of Lifetime Risk for Cardiovascular Disease by Risk Factor Burden at 50 Years of Age *Molecular Psychiatry.* 2006;113:791–798.

[3] International Headache Genetics Consortium , Gormley Padhraig, Anttila Verneri, et al. Meta-Analysis of 375,000 Individuals Identifies 38 Susceptibility Loci for Migraine *Nature Genetics.* 2016;48:856–866.

[4] Yang Jian, Zeng Jian, Goddard Michael E, Wray Naomi R, Visscher Peter M. Concepts, Estimation and Interpretation of SNP-based Heritability *Nature Genetics.* 2017;49:1304–1310.

[5] ADHD Working Group of the Psychiatric Genomics Consortium (PGC) , Early Lifecourse & Genetic Epidemiology (EAGLE) Consortium , 23andMe Research Team , et al. Discovery of the First Genome-Wide Significant Risk Loci for Attention Deficit/Hyperactivity Disorder *Nature Genetics.* 2019;51:63–75.

[6] Michailidou Kyriaki, Lindström Sara, Dennis Joe, et al. Association Analysis Identifies 65 New Breast Cancer Risk Loci *Nature.* 2017;551:92–94.

[7] Ferreira Manuel A.R., Mathur Riddhima, Vonk Judith M., et al. Genetic Architectures of Childhood- and Adult-Onset Asthma Are Partly Distinct *The American Journal of Human Genetics.* 2019;104:665–684.

[8] Hammerschlag Anke R, Stringer Sven, De Leeuw Christiaan A, et al. Genome-Wide Association Analysis of Insomnia Complaints Identifies Risk Genes and Genetic Overlap with Psychiatric and Metabolic Traits *Nature Genetics.* 2017;49:1584–1592.

[9] Takeuchi Fumihiko, Akiyama Masato, Matoba Nana, et al. Interethnic Analyses of Blood Pressure Loci in Populations of East Asian and European Descent *Nature Communications.* 2018;9:5052.

[10] Howitz Jette. Prevalence of Vitiligo: Epidemiological Survey on the Isle of Bornholm, Denmark *Archives of Dermatology.* 1977;113:47.

[11] Institute National Cancer. SEER*Explorer: An Interactive Website for SEER Cancer Statistics. Updated September 26, 2024.

[12] Dehlin Mats, Jacobsson Lennart, Roddy Edward. Global Epidemiology of Gout: Prevalence, Incidence, Treatment Patterns and Risk Factors *Nature Reviews Rheumatology.* 2020;16:380–390.

[13] Hittle Michael, Culpepper William J., Langer-Gould Annette, et al. Population-Based Estimates for the Prevalence of Multiple Sclerosis in the United States by Race, Ethnicity, Age, Sex, and Geographic Region *JAMA Neurology.* 2023;80:693.

[14] Pezzolo E, Cazzaniga S, Colombo P, Chatenoud L, Naldi L. Psoriasis Incidence and Lifetime Prevalence: Suggestion for a Higher Mortality Rate in Older Age-classes among Psoriatic Patients Compared to the General Population in Italy *Acta Dermato Venereologica.* 2019;99:400–403.

[15] Hadi Hazrina Ab, Tarmizi Aine Inani, Khalid Kamarul Ariffin, Gajdács Mário, Aslam Adeel, Jamshed Shazia. The Epidemiology and Global Burden of Atopic Dermatitis: A Narrative Review *Life.* 2021;11:936.

[16] Forss Anders, Clements Mark, Bergman David, et al. A Nationwide Cohort Study of the Incidence of Inflammatory Bowel Disease in Sweden from 1990 to 2014 *Alimentary Pharmacology & Therapeutics.* 2022;55:691–699.

[17] Kanis J. A., Johnell O., Oden A., et al. Long-Term Risk of Osteoporotic Fracture in Malmö *Osteoporosis International.* 2000;11:669–674.

[18] Lobo A., Lopez-Anton R., Santabárbara J., et al. Incidence and Lifetime Risk of Dementia and Alzheimer's Disease in a Southern European Population: Incidence and LTR of Dementia and AD *Acta Psychiatrica Scandinavica.* 2011;124:372–383.

[19] Institute National Eye. Glaucoma Data and Statistics: Glaucoma Tables https://www.nei.nih.gov/learn-about-eye-health/eye-health-data-and-statistics/glaucoma-data-and-statistics/glaucoma-tables.

[20] Bell Elizabeth J., Lutsey Pamela L., Basu Saonli, et al. Lifetime Risk of Venous Thromboembolism in Two Cohort Studies *The American Journal of Medicine.* 2016;129:339.e19-339.e26.

[21] Flohil Sophie C., Seubring Inge, Van Rossum Michelle M., Coebergh Jan-Willem W., De Vries Esther, Nijsten Tamar. Trends in Basal Cell Carcinoma Incidence Rates: A 37-Year Dutch Observational Study *Journal of Investigative Dermatology.* 2013;133:913–918.

[22] FinnGen . Hypertension – I9_HYPTENSESS https://risteys.finregistry.fi/endpoints/I9_HYPTENSESS 2024. FinnGen Risteys website. Accessed October 2024.

[23] Narayan K.M.V., Boyle James P., Thompson Theodore J., Gregg Edward W., Williamson David F.. Effect of BMI on Lifetime Risk for Diabetes in the U.S. *Diabetes Care.* 2007;30:1562–1566.

[24] Widen Erik, Lello Louis, Raben Timothy G., Tellier Laurent C. A. M., Hsu Stephen D. H.. Polygenic Health Index, General Health, and Pleiotropy: Sibling Analysis and Disease Risk Reduction *Scientific Reports.* 2022;12:18173.

[25] Prediction Genomic. Risk Reduction Calculator https://www.lifeview.com/risk-reduction-calculator.

[26] Orchid Health . Whitepapers https://guides.orchidhealth.com/category/whitepapers.

[27] Folkersen Lasse. Impute-Me: PRS Directory https://github.com/spartahawk/impute-me/tree/master/prs 2021.

[28] Saha Rama, Pettersson Hans Järnbert, Svedberg Pia, et al. Heritability of Endometriosis *Fertility and Sterility.* 2015;104:947–952.

[29] Vink J. M., Sadrzadeh S., Lambalk C. B., Boomsma D. I.. Heritability of Polycystic Ovary Syndrome in a Dutch Twin-Family Study *The Journal of Clinical Endocrinology & Metabolism.* 2006;91:2100–2104.